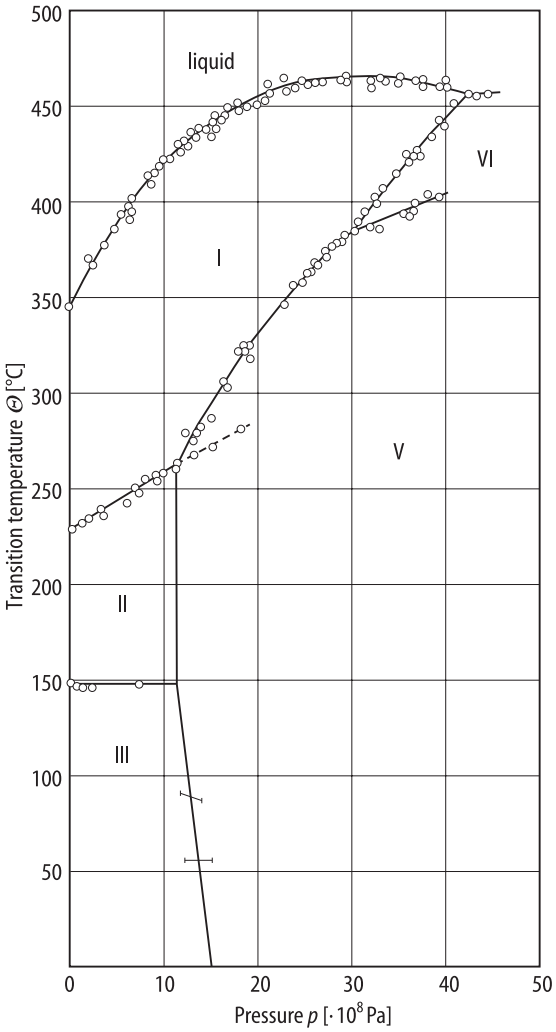

Fig. 33A-3-001. CsH_2PO_4 (CDP). Phase diagram [78Rap]. Dashed line: metastable extension.

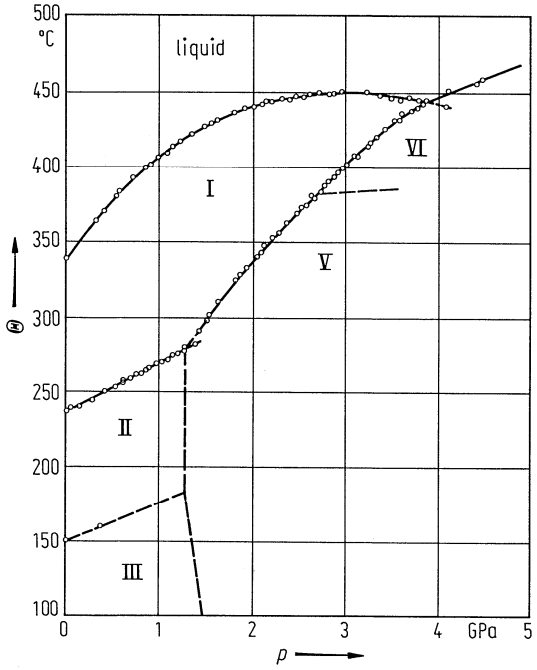

Fig. 33A-3-002. CsD_2PO_4 (DCDP). Phase diagram [81Kin].

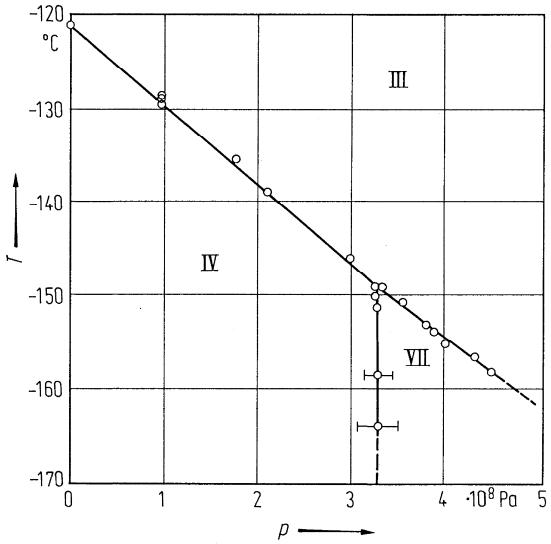

Fig. 33A-3-003. CsH_2PO_4 (CDP). Phase diagram [78Yas], see also [78Ges].

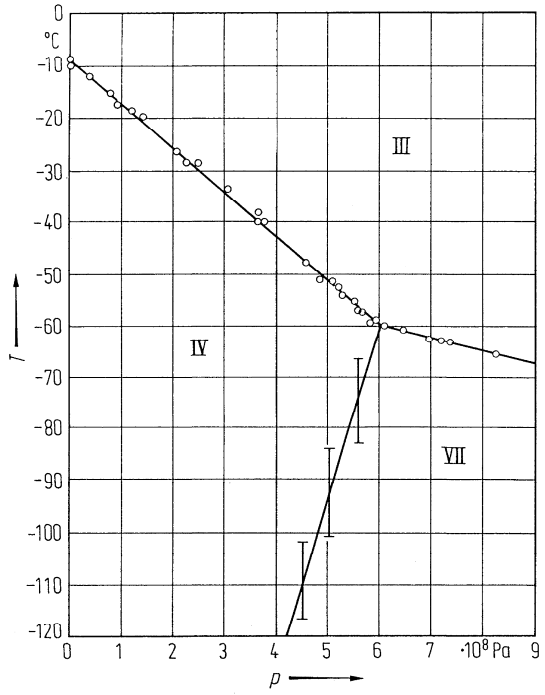

Fig. 33A-3-004. CsD_2PO_4 (DCDP). Phase diagram [78Ges]. Θ_f at $p = 0$ is –8.5 °C.

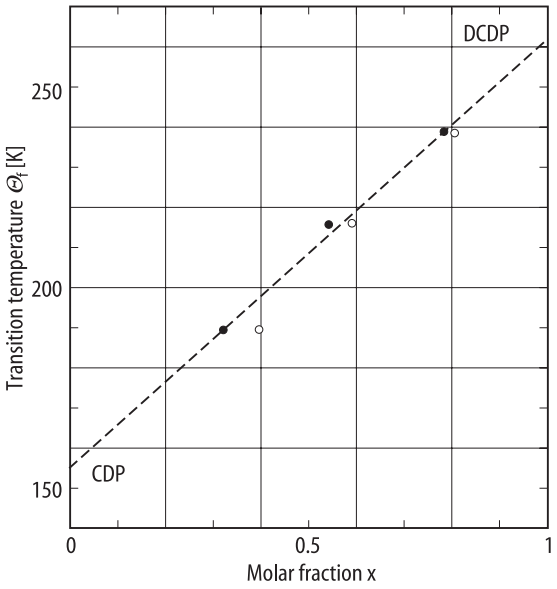

Fig. 33A-3-005. $CsH_{2(1-x)}D_{2x}PO_4$. Θ_f vs. x [94Iwa]. The deuteration rates of two crystallographically nonequivalent hydrogen bonds are determined by neutron diffraction. Open circle: H(1), full circle: H(2). H(1): hydrogen atom in the longer hydrogen bond connecting PO_4 group perpendicular to the *b* axis. H(2): hydrogen atom in the shorter hydrogen bond connecting PO_4 groups along the *b* axis. See Fig. 33A-3-009.

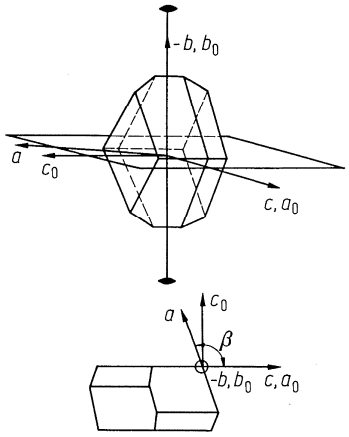

Fig. 33A-3-006. CsH_2PO_4 (CDP). Crystal form [76Ues]. *a*, *b*, *c*: crystallographic axes in monoclinic system; a_o, b_o, c_o: those assigned as orthorhombic system in [52Fel] and those assigned as pseudo-orthorhombic system in [78Nel].

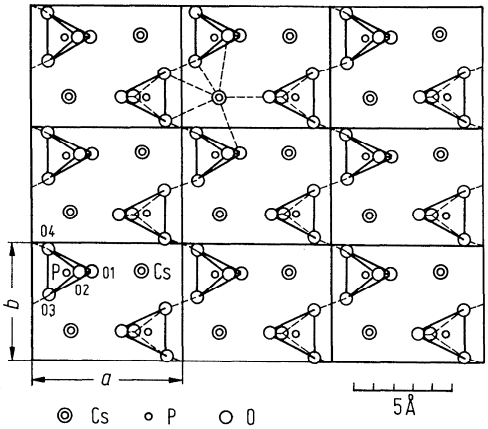

Fig. 33A-3-007. CsH_2PO_4 (CDP). Structure of phase III [76Ues]. Projection on (001) plane.

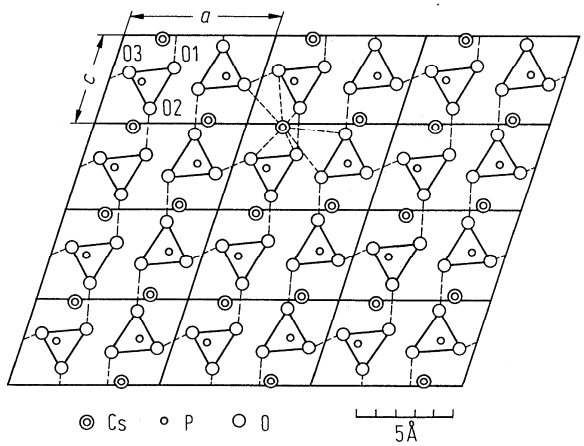

Fig. 33A-3-008. CsH_2PO_4 (CDP). Structure of phase III [76Ues]. Projection on (010) plane.

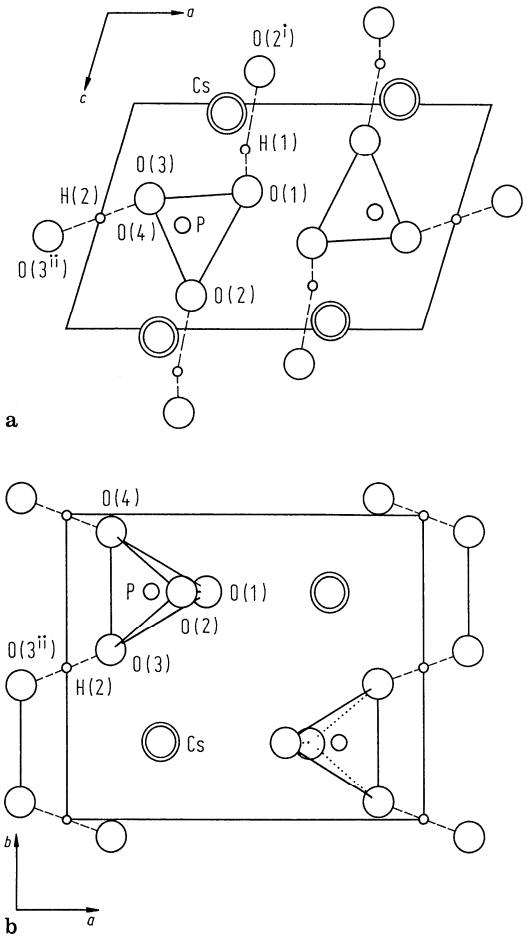

Fig. 33A-3-009. CsH_2PO_4 (CDP). Structure of phase III [80Mat]. (**a**) View along the *b* axis and (**b**) along the *c* axis.

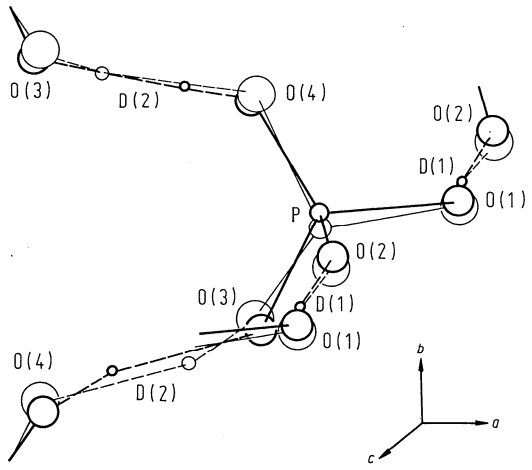

Fig. 33A-3-010. CsD_2PO_4 (DCDP). A view of the disordered structure in phase III [83Ito]. Thick and thin lines correspond to the two sets of the equillibrium configurations.

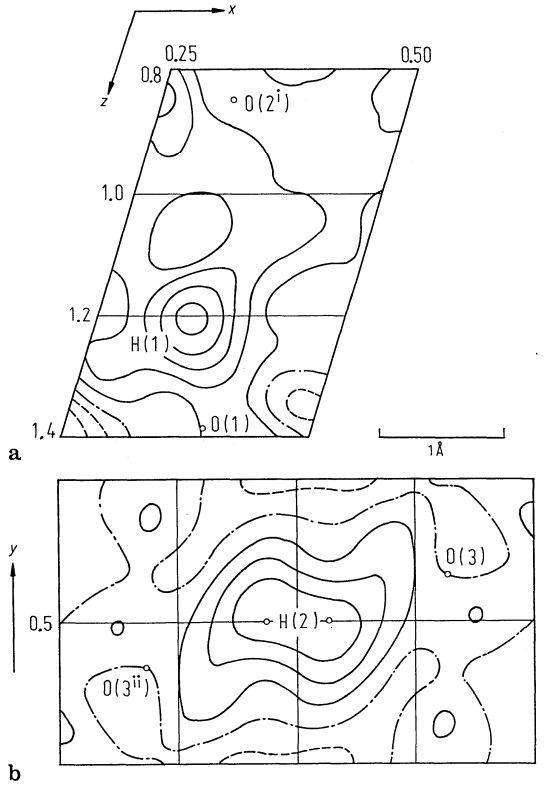

Fig. 33A-3-011. CsH_2PO_4 (CDP). Electron density map of H atoms at RT [80Mat].The interval of contours is 0.2 eÅ^{-3} (**a**) around H(1), (**b**) around H(2).

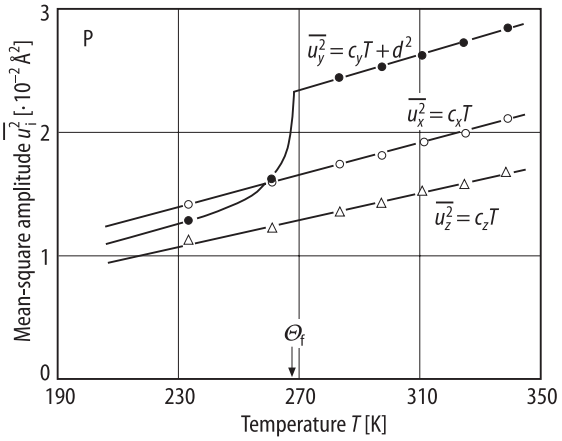

Fig. 33A-3-012. CsD_2PO_4 (DCDP). $\overline{u_i^2}$ vs. T for P atom [83Ito]. $\overline{u_i^2}$ (i = x, y, z): mean-square thermal amplitude. c_x, c_y, c_z, d: fitting parameters for the data above Θ_f.

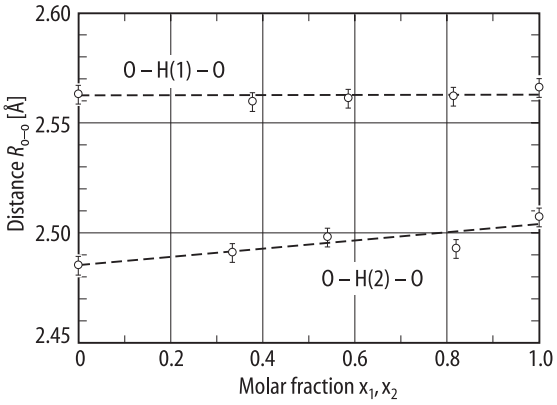

Fig. 33A-3-013. $CsH_{2(1-x)}D_{2x}PO_4$. R_{O-O} vs. x_1, x_2 [94Iwa]. T = 80 K. R_{O-O}: O–O distance of the hydrogen bond. x_1, x_2: deuteration rates of H(1), H(2) sites, respectively. H(1), H(2): see the caption of Fig. 33A-3-005.

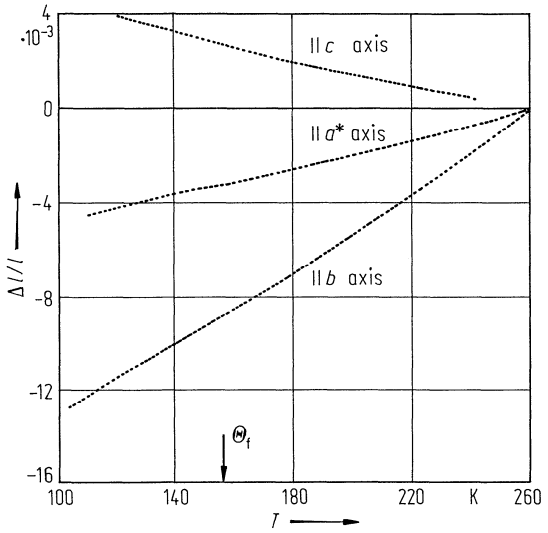

Fig. 33A-3-014. CsH_2PO_4 (CDP). $\Delta l/l$ vs. T [84Deg2]. $\Delta l/l$: linear thermal expansion.

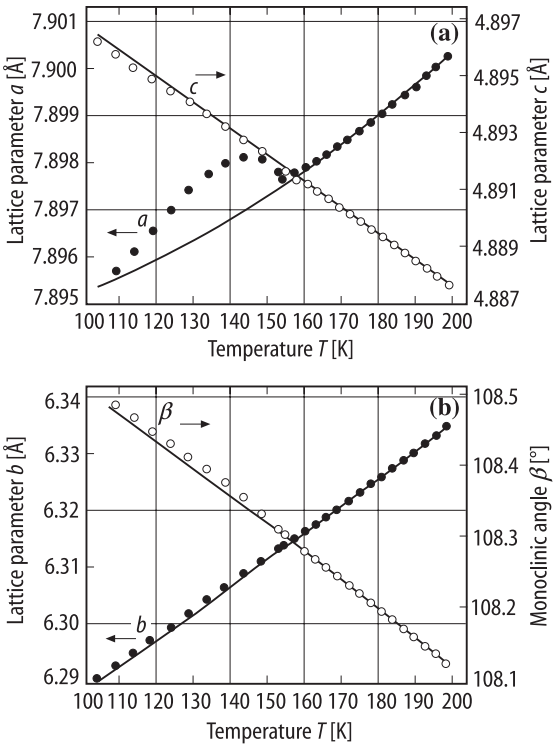

Fig. 33A-3-015. CsH_2PO_4 (CDP). a, b, c, β vs. T from 100 K to 200 K [93Bro]. (**a**) a, c. (**b**) b, β. Full line: calculated values by means of polynomial approximation for the data above Θ_t.

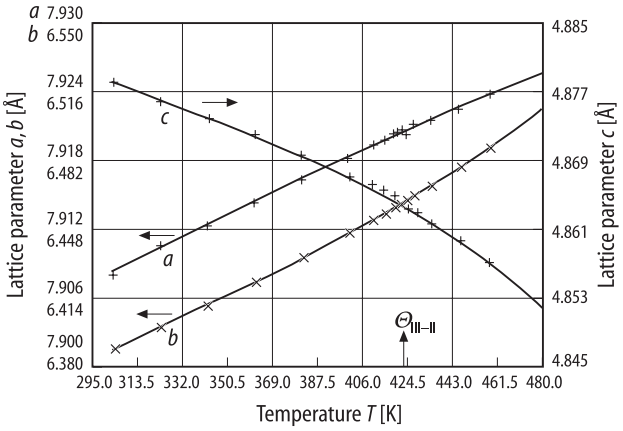

Fig. 33A-3-016. CsH_2PO_4 (CDP). a, b, c vs. T above RT [90Bro].

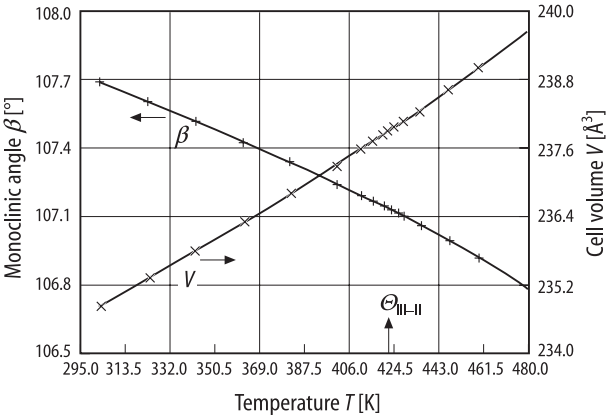

Fig. 33A-3-017. CsH_2PO_4 (CDP). β, V vs. T above RT [90Bro]. β: monoclinic angle. V: volume of unit cell.

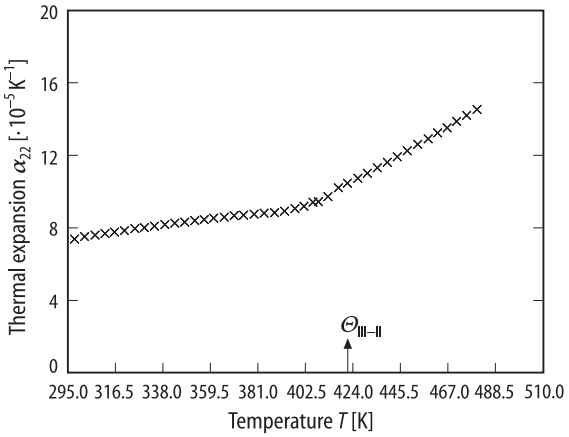

Fig. 33A-3-018. CsH_2PO_4 (CDP). α_{22} vs. T above RT [90Bro]. α_{22}: linear thermal expansion coefficient.

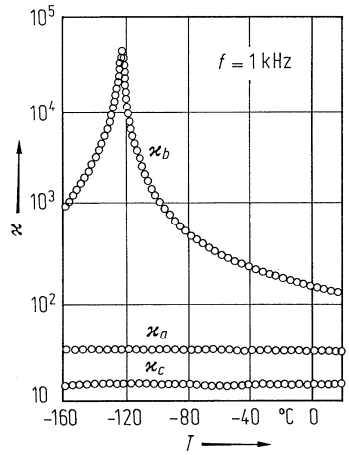

Fig. 33A-3-019. CsH_2PO_4 (CDP). κ_a, κ_b, κ_c vs. T [76Ues]. f = 1 kHz.

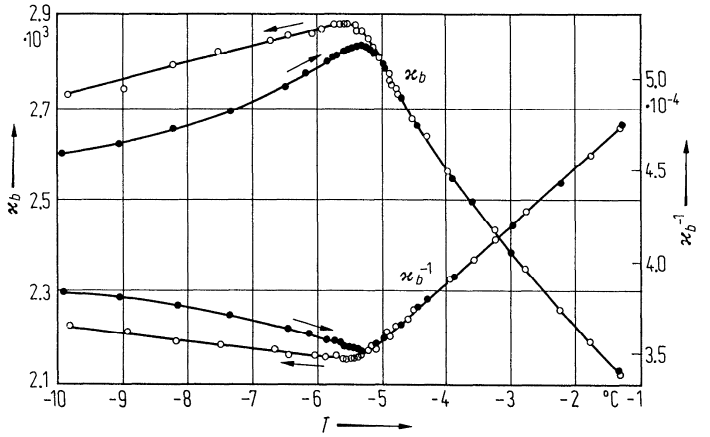

Fig. 33A-3-020. CsD_2PO_4 (DCDP). $\varkappa_b$, $\varkappa_b^{-1}$ vs. T [75Lev]. Deuteration degree is more than 90%. f = 1 kHz.

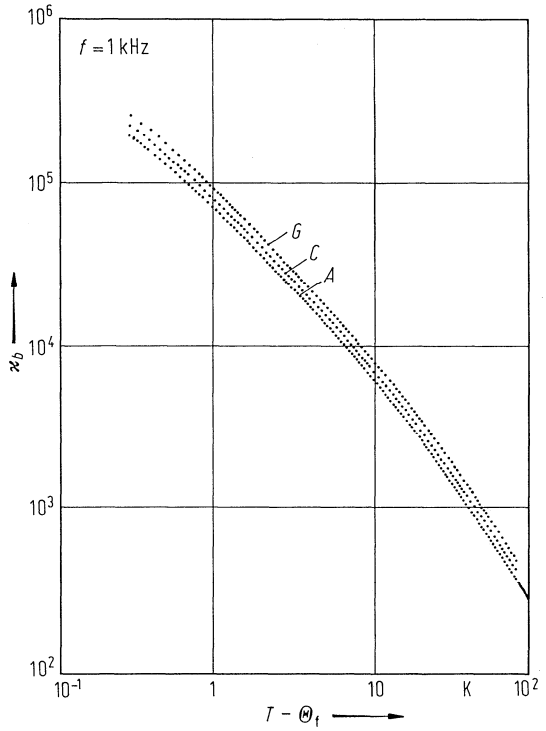

Fig. 33A-3-021. $CsH_{2(1-x)}D_{2x}PO_4$. $\varkappa_b$ vs. $T - \Theta_f$ at 1 kHz [82Deg]. *A*: x = 0, *C*: x = 0.14, *G*: x = 0.98. Relation between Θ_f and x: see the caption of Fig. 33A-3-022.

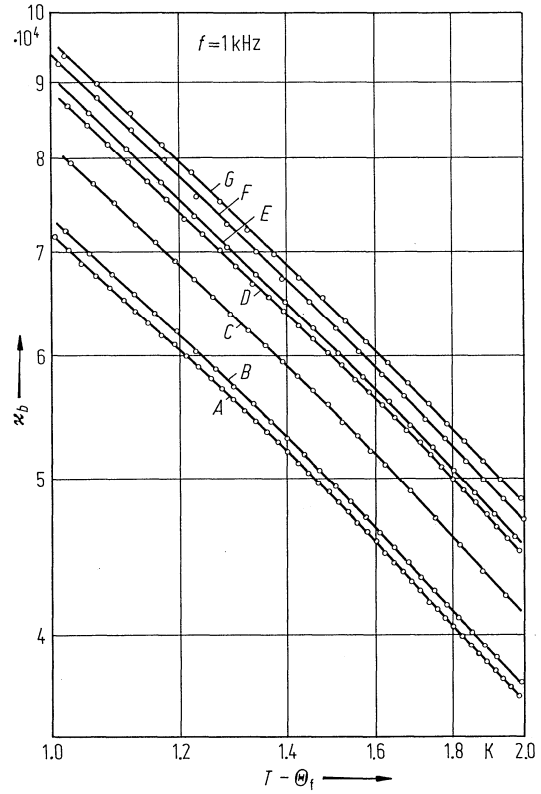

Fig. 33A-3-022. $CsH_{2(1-x)}D_{2x}PO_4$. κ_b vs. $T - \Theta_f$ at 1 kHz [82Deg]. Curve *A*: x = 0, Θ_f = 156.0 K; *B*: 0.03, 159.3 K; *C*: 0.14, 172.0 K; *D*: 0.27, 186.6 K; *E*: 0.48, 211.4 K; *F*: 0.65, 230.9 K; *G*: 0.98, 268.3 K.

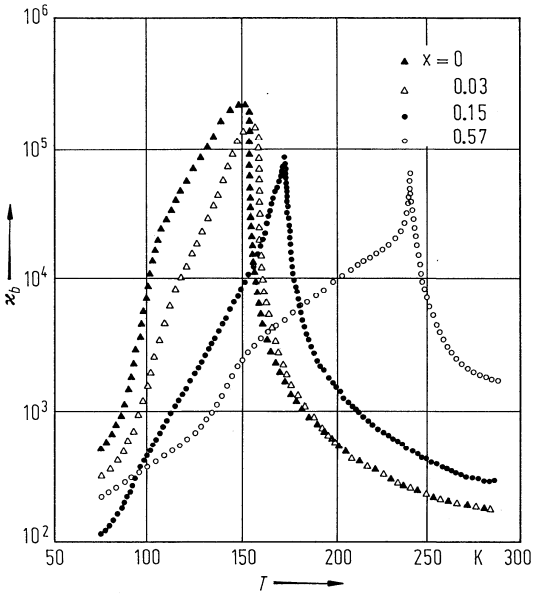

Fig. 33A-3-023. $CsH_{2(1-x)}D_{2x}PO_4$. κ_b vs. T [80Bar]. Parameter: x.

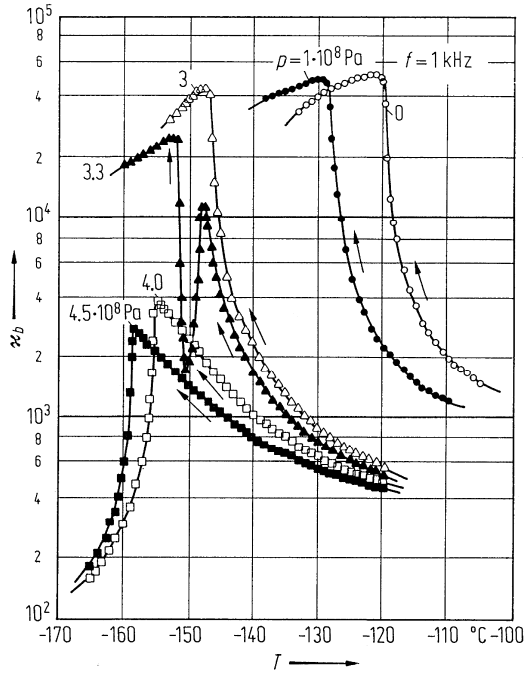

Fig. 33A-3-024. CsH_2PO_4 (CDP). κ_b vs. T [78Yas]. Parameter: p.

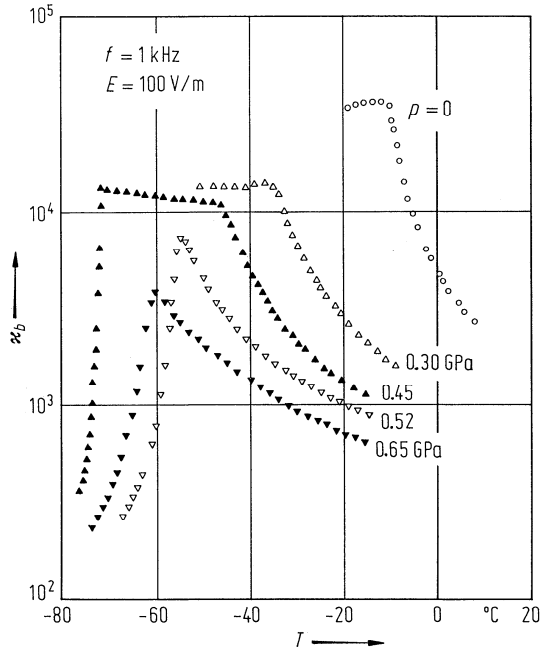

Fig. 33A-3-025. CsD_2PO_4 (DCDP). κ_b vs. T [79Yas1]. Parameter: p.

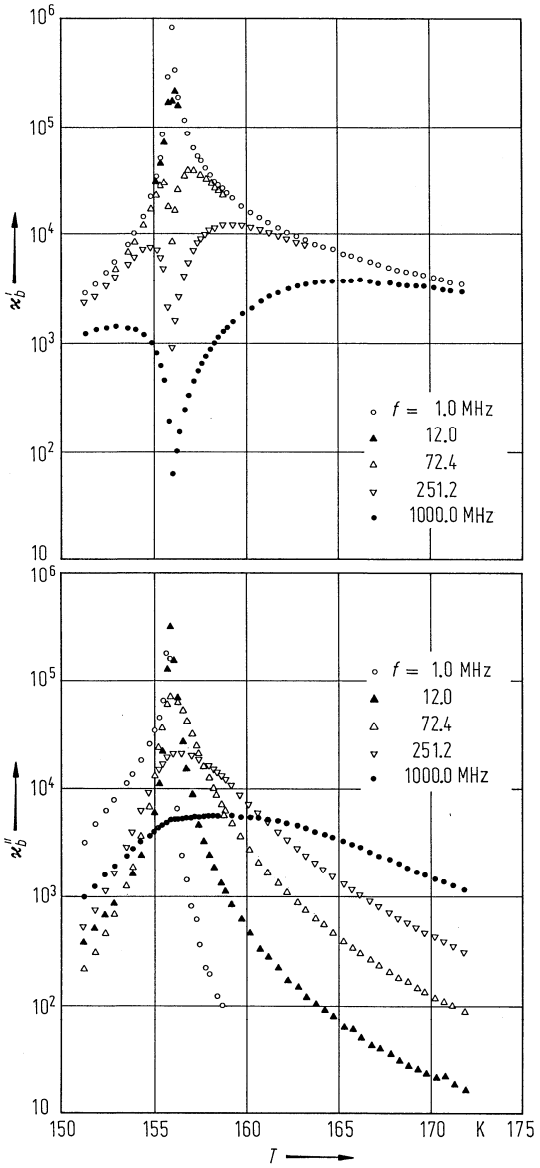

Fig. 33A-3-026. CsH_2PO_4 (CDP). κ_b', κ_b'' vs. T [82Deg]. Parameter: f.

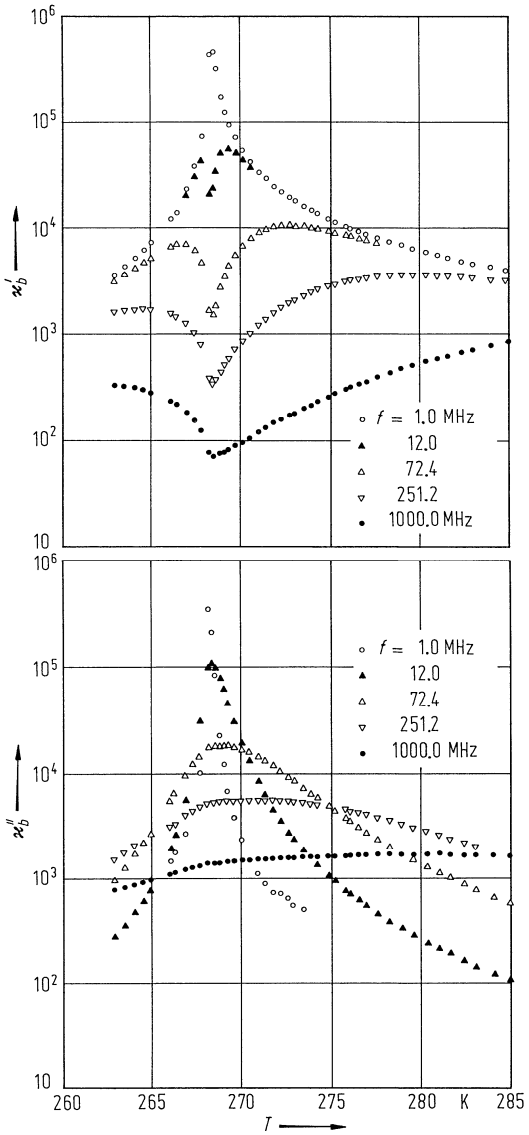

Fig. 33A-3-027. CsD_2PO_4 (DCDP). κ_b', κ_b'' vs. T [82Deg]. Parameter: f. Deuteration rate: 0.97.

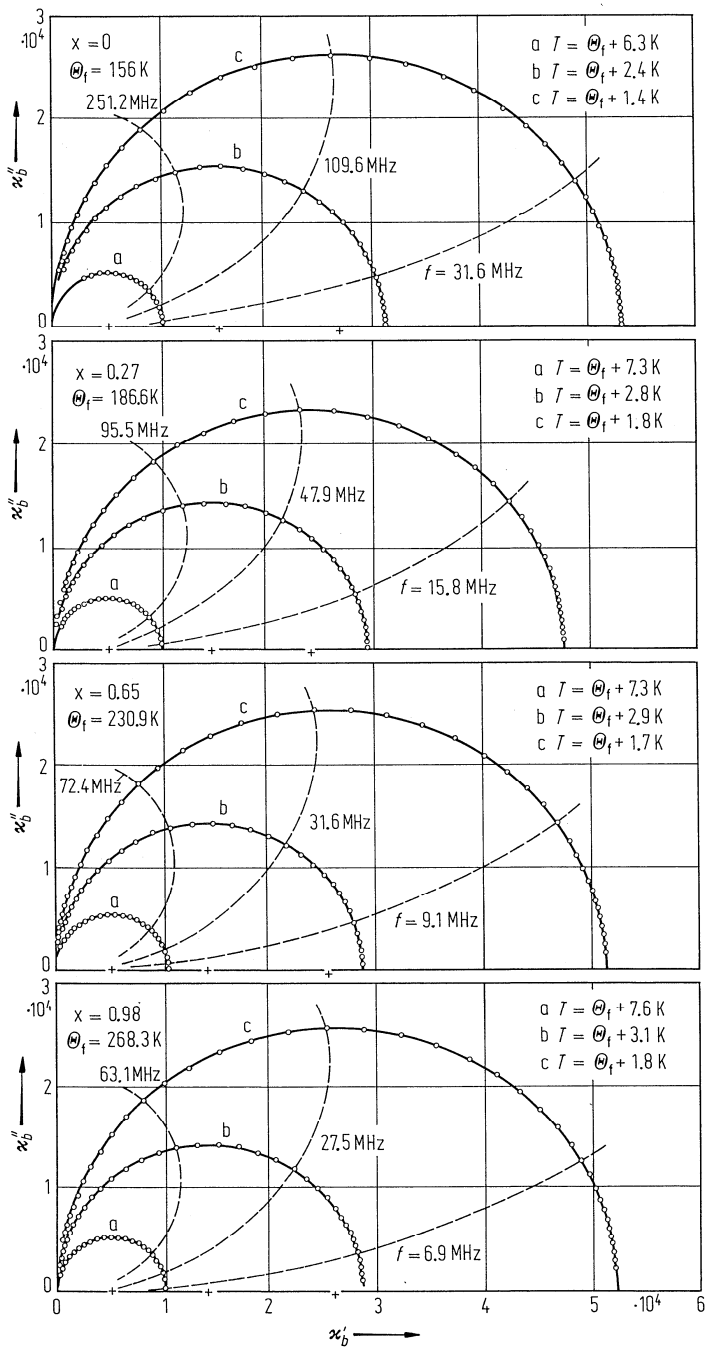

Fig. 33A-3-028. $CsH_{2(1-x)}D_{2x}PO_4$. κ_b' vs. κ_b'' (Cole-Cole diagram) above Θ_f [82Deg]. Parameters: x, *T*. Plus sign: centers of circular arcs.

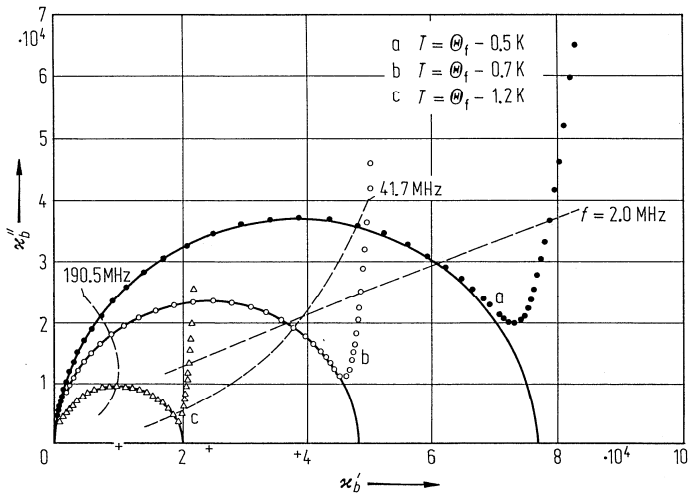

Fig. 33A-3-029. CsH_2PO_4 (CDP). κ_b' vs. κ_b'' (Cole-Cole diagram) below Θ_f [82Deg]. Parameter: T. Plus sign: centers of circular arcs.

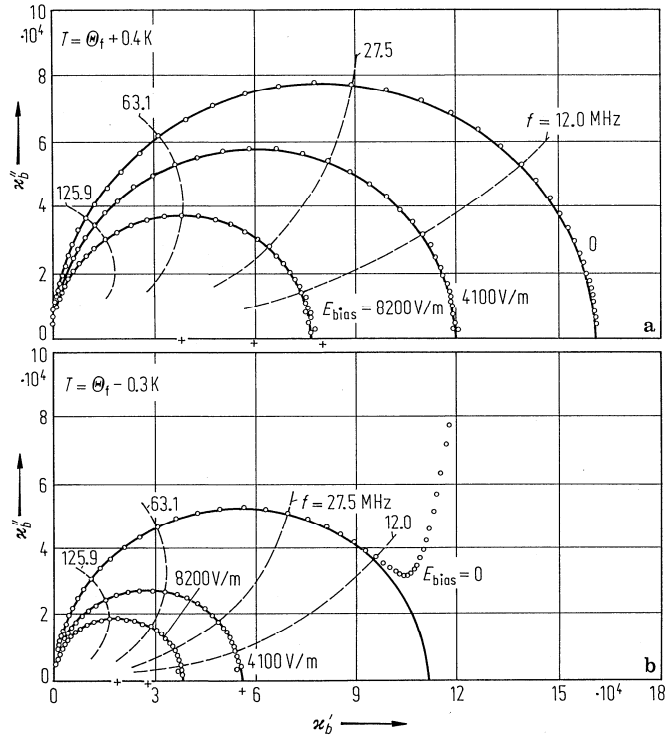

Fig. 33A-3-030. CsH_2PO_4 (CDP). κ_b' vs. κ_b'' (Cole-Cole diagram) [82Deg]. Parameter: E_{bias}. E_{bias}: dc bias field. Plus sign: centers of circular arcs. (**a**) $T = \Theta_f + 0.4$ K, (**b**) $T = \Theta_f - 0.3$ K.

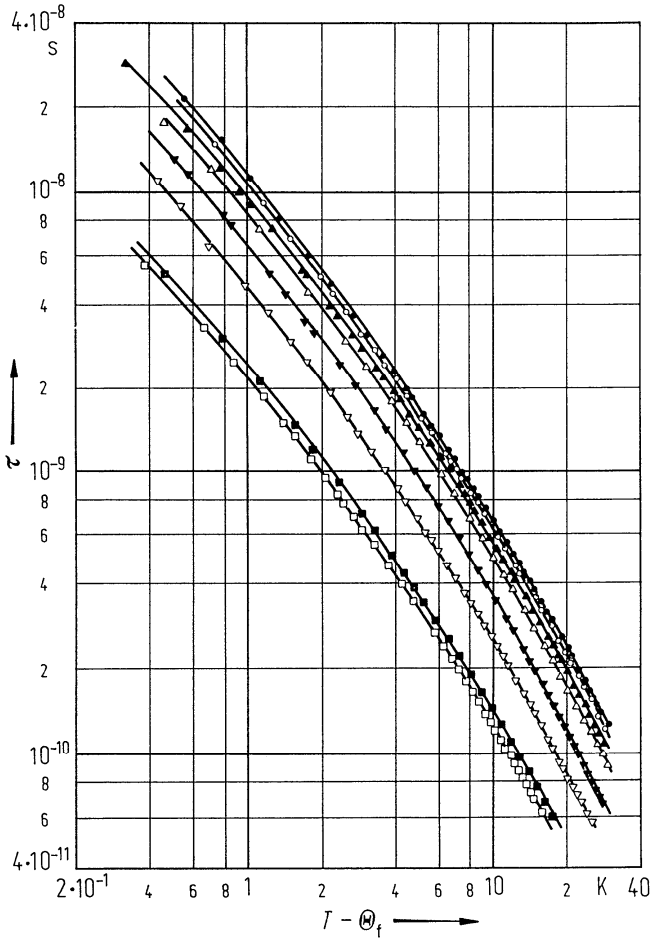

Fig. 33A-3-031. $CsH_{2(1-x)}D_{2x}PO_4$. τ vs. $T - \Theta_f$ [82Deg]. Parameter: x. τ: relaxation time of dielectric dispersion.

	open square	full square	open downside triangle	full downside triangle	open upside triangle	full upside triangle	open circle	full circle
x	0	0.03	0.14	0.27	0.48	0.65	0.82	0.98
Θ_f [K]	156.0	159.3	172.0	186.6	211.4	230.9	249.8	268.3

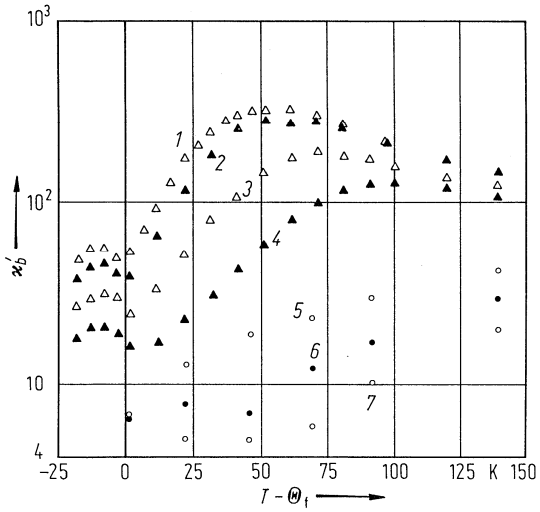

Fig. 33A-3-032. $CsH_{2(1-x)}D_{2x}PO_4$. κ_b' vs. $T - \Theta_f$ [86Lev]. Parameter: *f. 1*: 18.7 GHz, *2*: 22.5 GHz, *3*: 30.7 GHz, *4*: 45.0 GHz, *5*: 189.0 GHz, *6*: 278.9 GHz, *7*: 375 GHz; *1*…*4*: x = 0; *5*…*7*: x = 0.03.

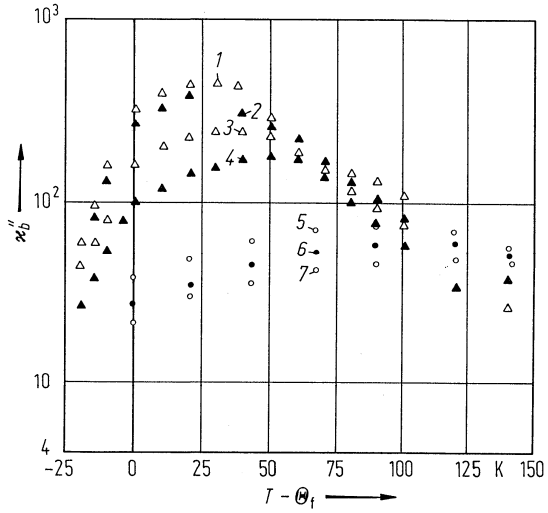

Fig. 33A-3-033. $CsH_{2(1-x)}D_{2x}PO_4$. κ_b'' vs. $T - \Theta_f$ [86Lev]. Parameter: *f*. Symbols are the same as in Fig. 33A-3-032.

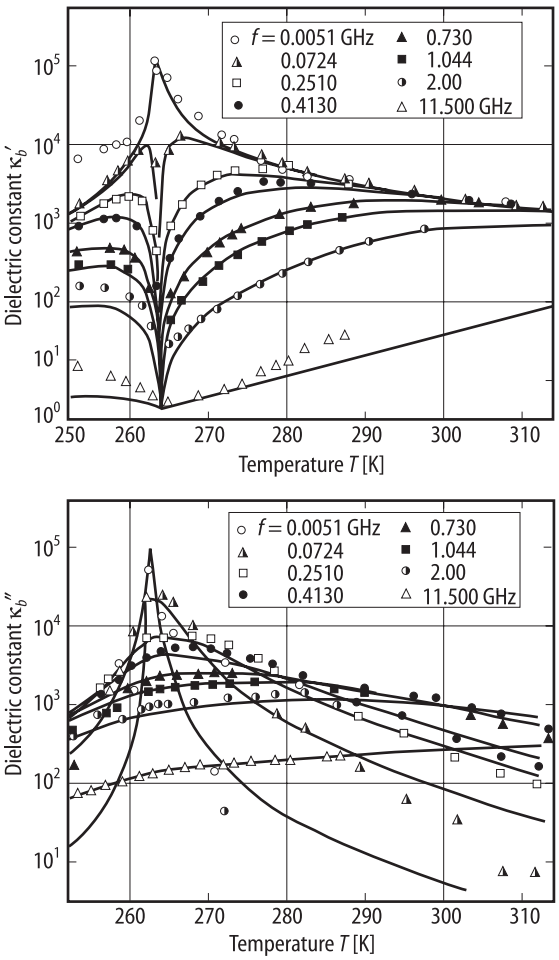

Fig. 33A-3-034. CsD_2PO_4 (DCDP). κ_b', κ_b'' vs. T [88Gri]. Parameter: f.

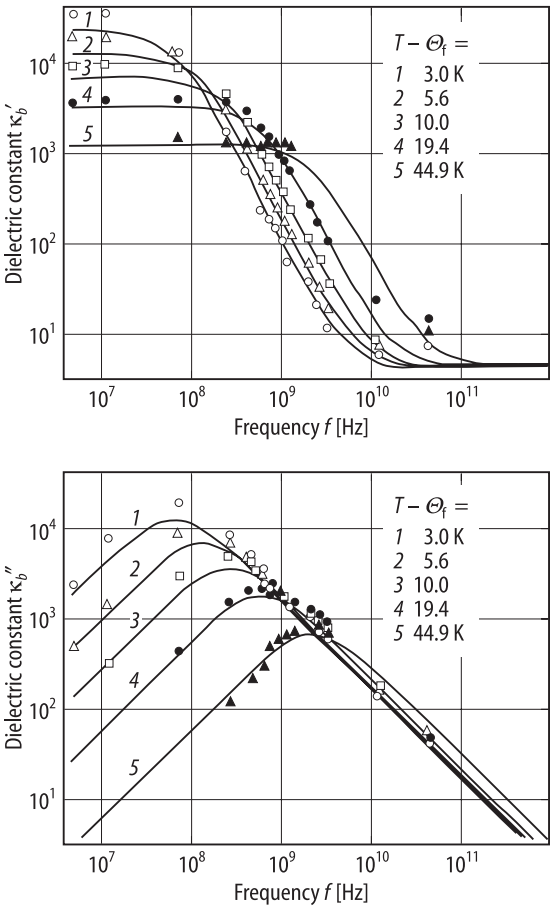

Fig. 33A-3-035. CsD_2PO_4 (DCDP). κ_b', κ_b'' vs. f [88Gri]. Parameter: $T - \Theta_f$.

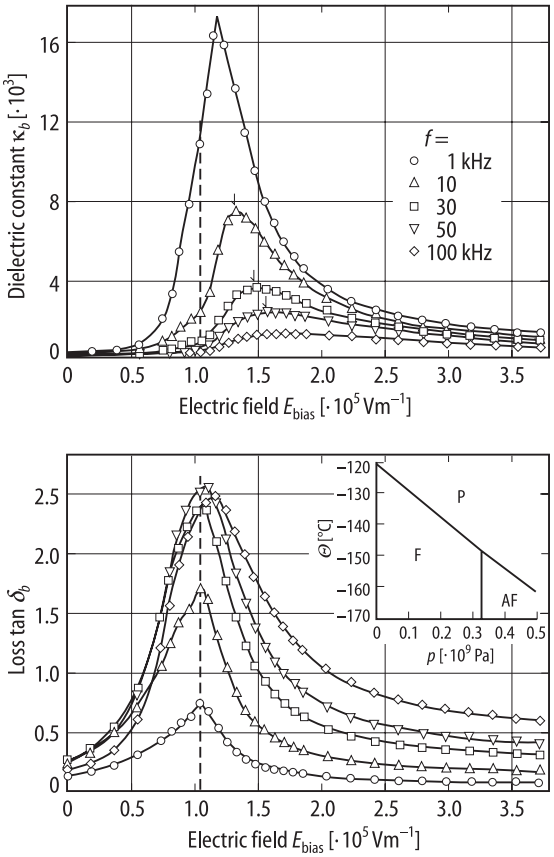

Fig. 33A-3-036. CsH_2PO_4 (CDP). κ_b, $\tan\delta_b$ vs. E_{bias} at $T = -170$ °C, $p = 0.45$ GPa [90Yas]. Parameter: *f*. Insert shows Θ vs. *p* phase diagram.

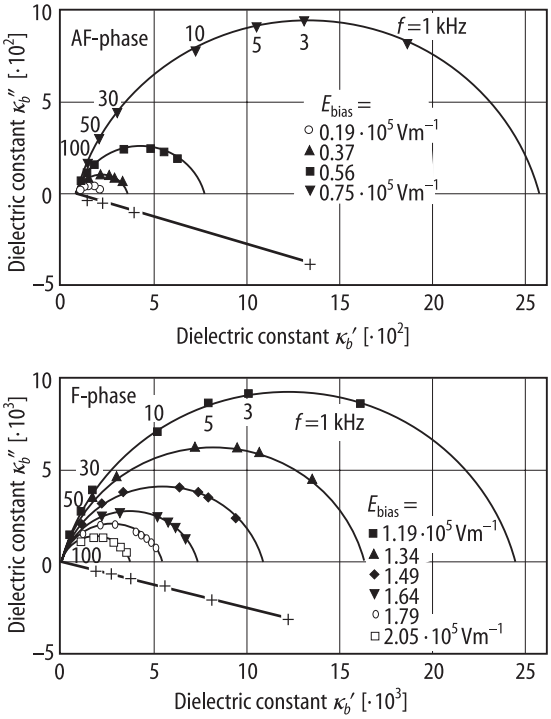

Fig. 33A-3-037. CsH_2PO_4 (CDP). κ_b'' vs. κ_b' (Cole-Cole diagram) [90Yas]. Parameter: E_{bias}. $T = -170$ °C, $p = 0.45$ GPa. Plus sign: centers of arcs.

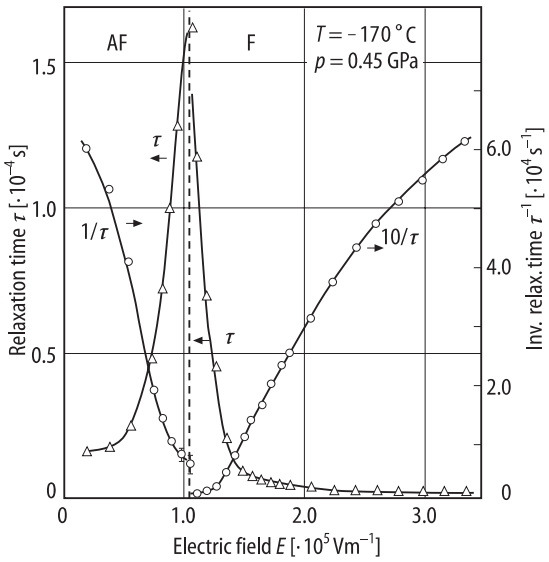

Fig. 33A-3-038. CsH_2PO_4 (CDP). τ, $1/\tau$ vs. E [90Yas]. τ: dielectric relaxation time. $T = -170$ °C, $p = 0.45$ GPa.

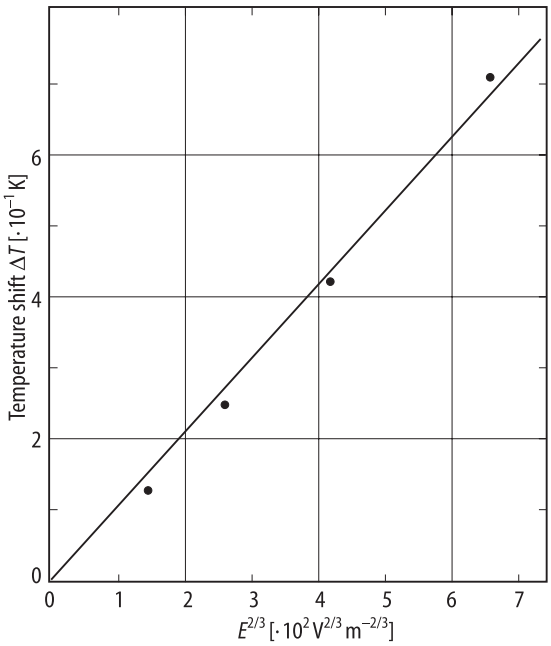

Fig. 33A-3-039. CsH_2PO_4 (CDP). ΔT vs. $E^{2/3}$ [93Ani]. $\Delta T = T_{max} - \Theta_f$. T_{max}: temperature of maximum dielectric constant.

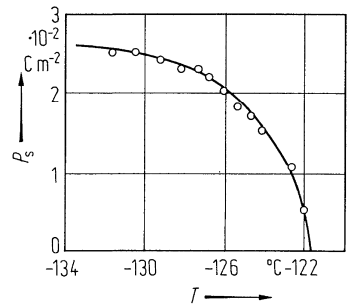

Fig. 33A-3-040. CsH_2PO_4 (CDP). P_s vs. T [76Ues].

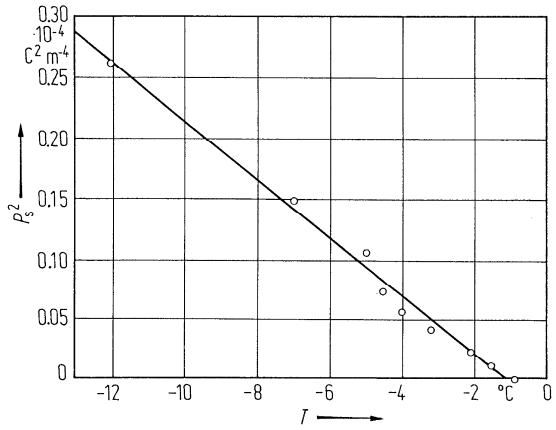

Fig. 33A-3-041. CsD_2PO_4 (DCDP). P_s^2 vs. T [75Lev].

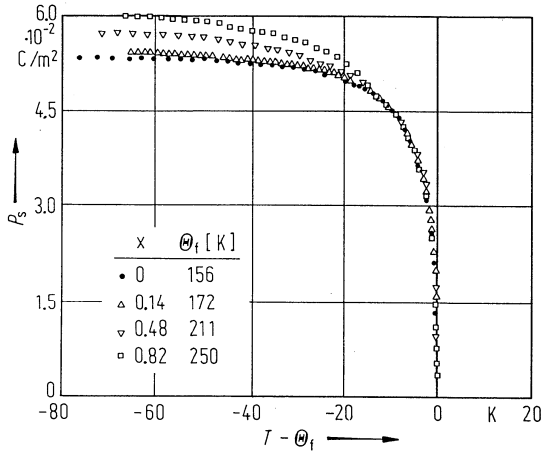

Fig. 33A-3-042. $CsH_{2(1-x)}D_{2x}PO_4$. P_s vs. $T - \Theta_f$ [82Deg]. Parameter: x.

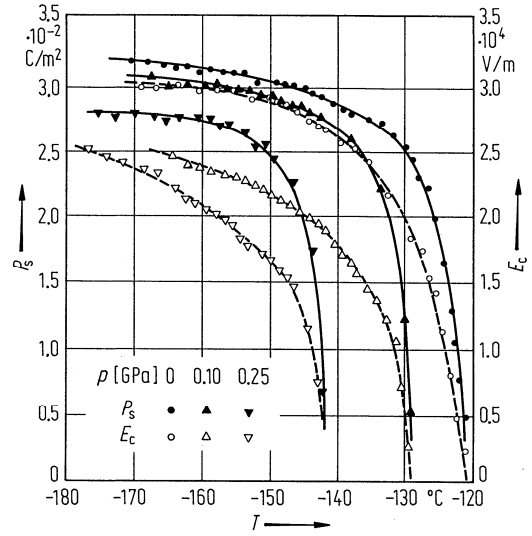

Fig. 33A-3-043. CsH_2PO_4 (CDP). P_s, E_c vs. T [79Yas1]. Parameter: p.

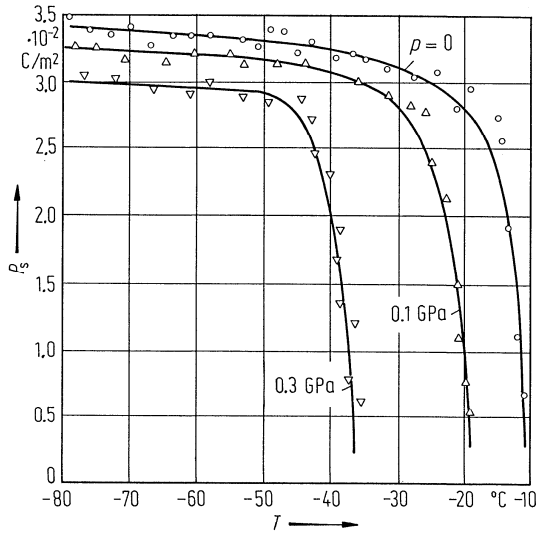

Fig. 33A-3-044. CsD_2PO_4 (DCDP). P_s vs. T [79Yas1]. Parameter: p.

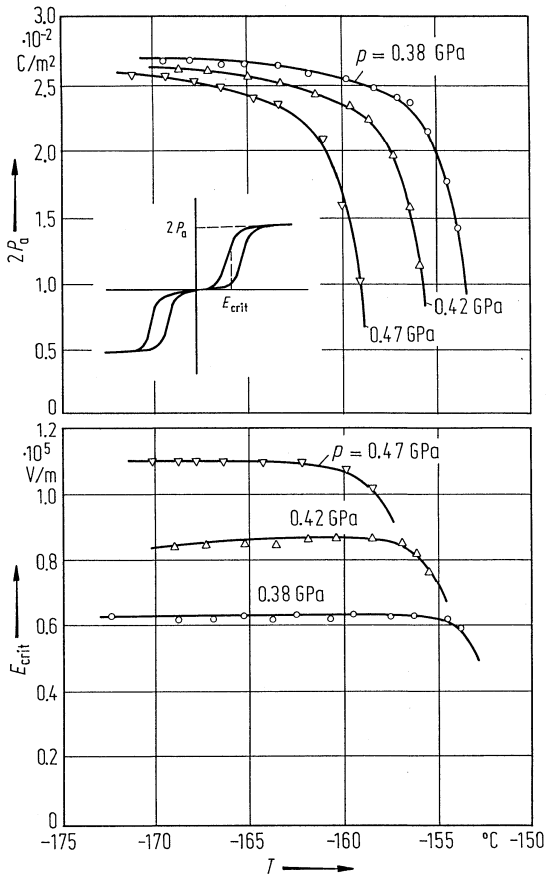

Fig. 33A-3-045. CsH_2PO_4 (CDP). $2P_a$, E_{crit} vs. T in the antiferroelectric phase VII [79Yas1]. Parameter: p. P_a: sublattice polarization, E_{crit}: critical field.

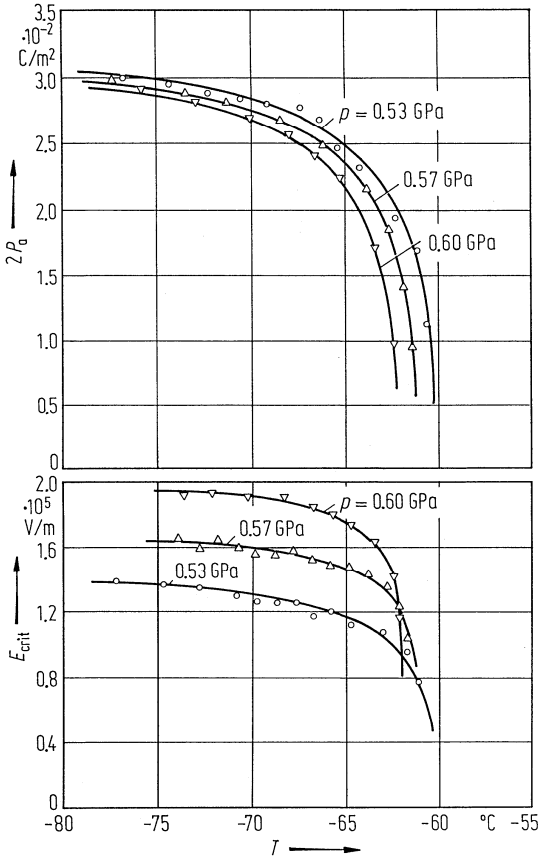

Fig. 33A-3-046. CsD_2PO_4 (DCDP). $2P_a$, E_{crit} vs. T in the antiferroelectric phase VII [79Yas1]. Parameter: p. P_a: sublattice polarization, E_{crit}: critical field. See inset of Fig. 33A-3-045.

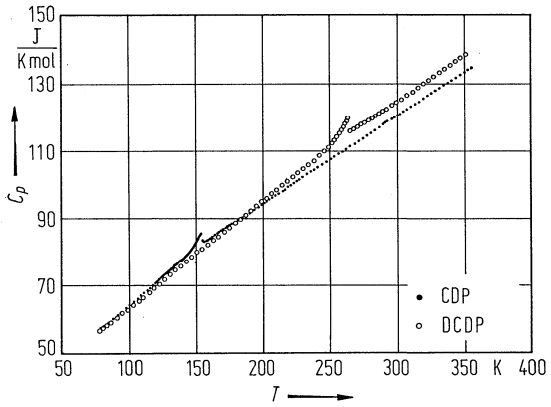

Fig. 33A-3-047. CsH_2PO_4 (CDP), CsD_2PO_4 (DCDP). C_p vs. T [83Ima]. C_p: molar heat capacity at constant pressure.

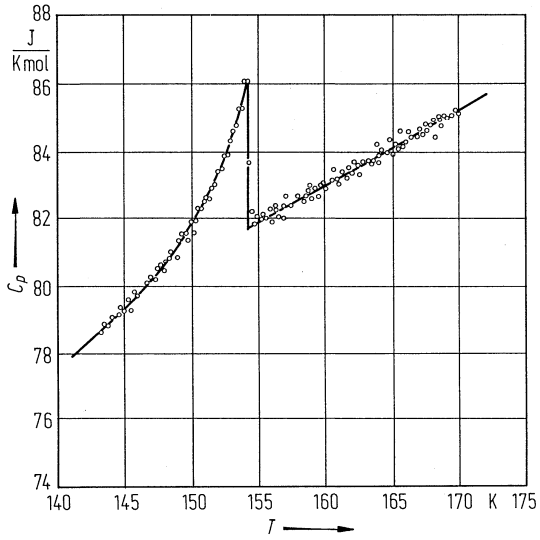

Fig. 33A-3-048. CsH_2PO_4 (CDP). C_p vs. T near Θ_f [83Ima]. C_p: molar heat capacity at constant pressure.

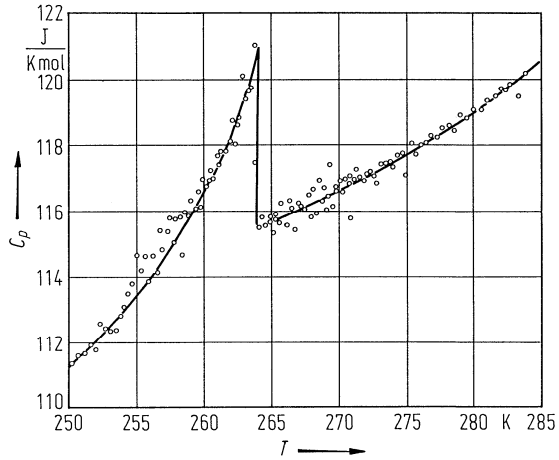

Fig. 33A-3-049. CsD_2PO_4 (DCDP). C_p vs. T near Θ_f [83Ima]. C_p: molar heat capacity at constant pressure.

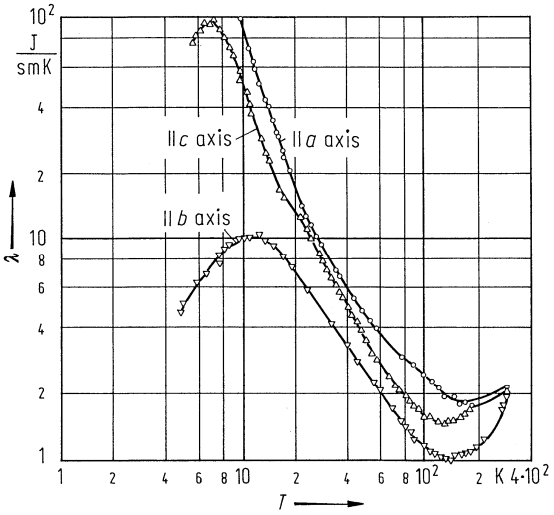

Fig. 33A-3-050. CsH_2PO_4 (CDP). λ vs. T [84Spo]. λ: thermal conductivity.

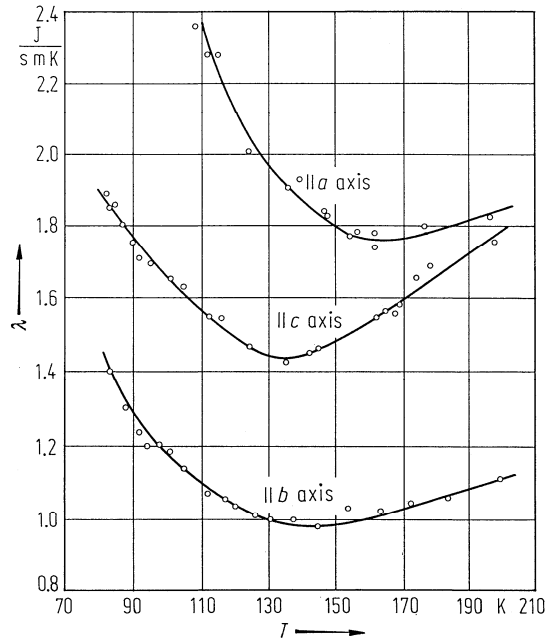

Fig. 33A-3-051. CsH_2PO_4 (CDP). λ vs. T near Θ_f [84Spo]. λ: thermal conductivity.

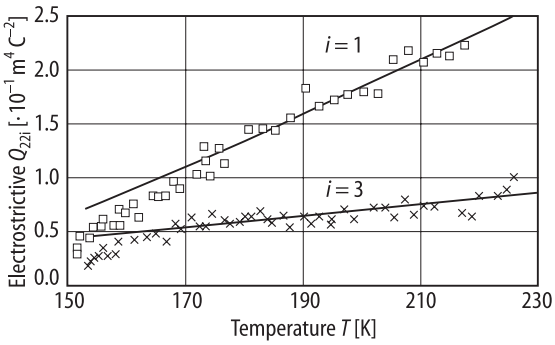

Fig. 33A-3-052. CsH_2PO_4 (CDP). Q_{22i} vs. T [90Sor]. Q_{22i}: electrostrictive constant measured by piezoelectric resonance method.

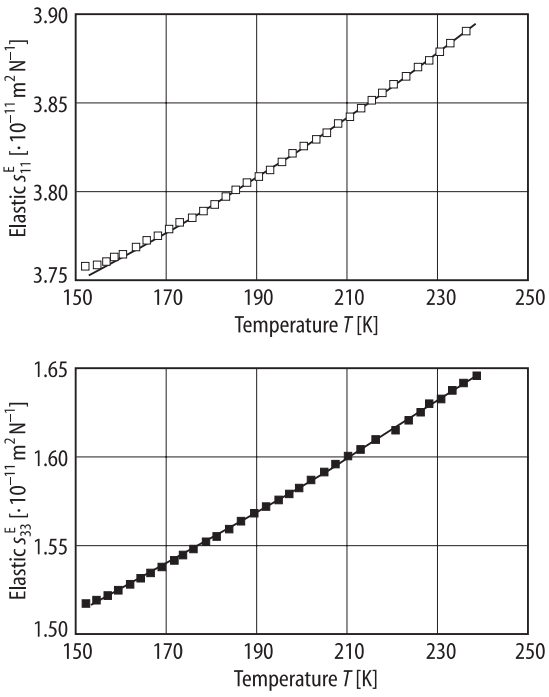

Fig. 33A-3-053. CsH_2PO_4 (CDP). $s_{11}^{\boldsymbol{E}}$, $s_{33}^{\boldsymbol{E}}$ vs. T [90Sor]. $s_{11}^{\boldsymbol{E}}$, $s_{33}^{\boldsymbol{E}}$: elastic compliances measured by piezoelectric resonance method.

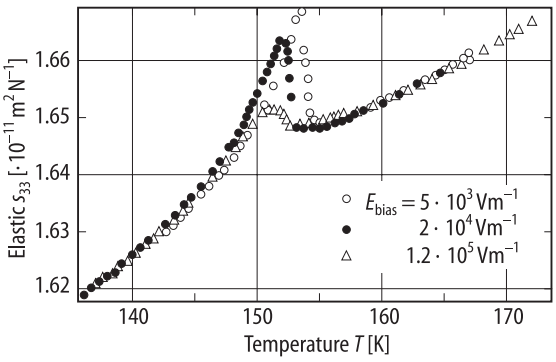

Fig. 33A-3-054. CsH_2PO_4 (CDP). s_{33} vs. T [88Sor]. Parameter: E_{bias}.

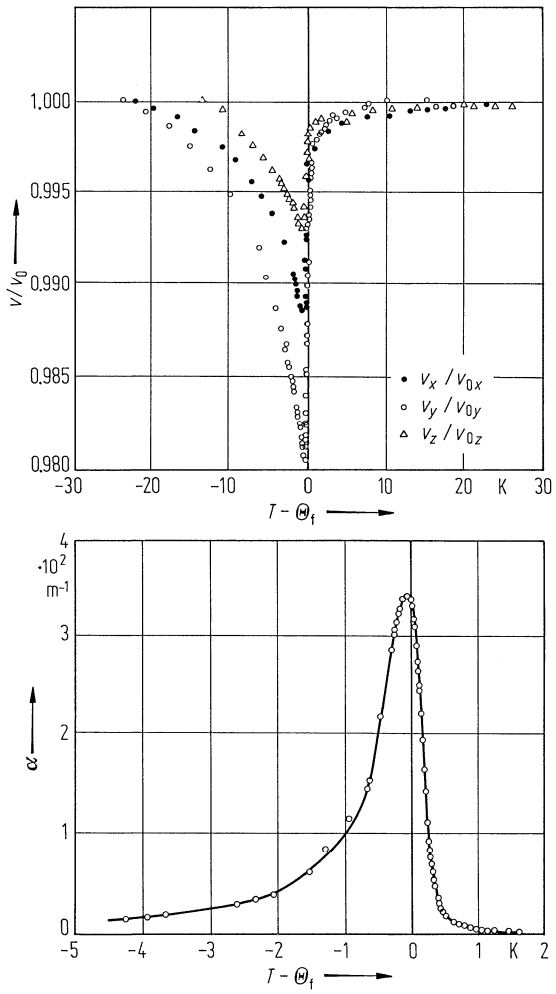

Fig. 33A-3-055. CsH_2PO_4 (CDP). v/v_0, α vs. $T - \Theta_f$ for longitudinal sound wave [81Yak]. f = 10 MHz. v_x/v_{0x}, v_y/v_{0y}, v_z/v_{0z}: relative sound velocities propagating along the a^*, b, c axes, respectively ($\boldsymbol{a^*} \parallel \boldsymbol{b} \times \boldsymbol{c}$). α: absorption coefficient of the sound wave propagating along the b axis.

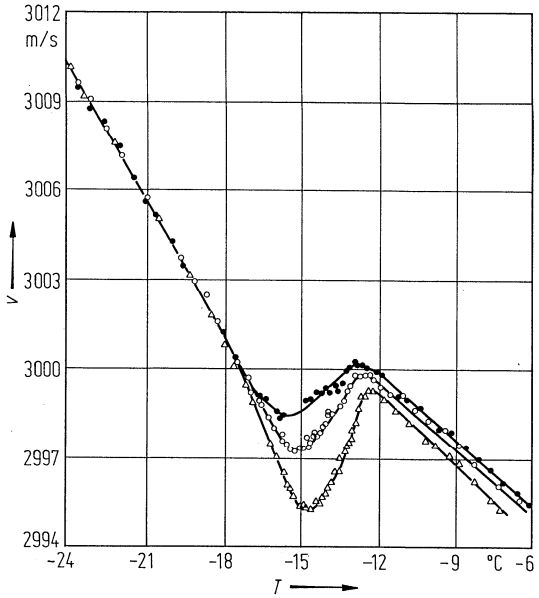

Fig. 33A-3-056. CsD_2PO_4 (DCDP). υ vs. T [82Kas]. Parameter: *f.* υ: velocity of longitudinal sound wave propagating along the a^* axis ($\boldsymbol{a}^* \parallel \boldsymbol{b} \times \boldsymbol{c}$). Open upside triangle: 10 MHz, open circle: 30 MHz, full circle: 50 MHz.

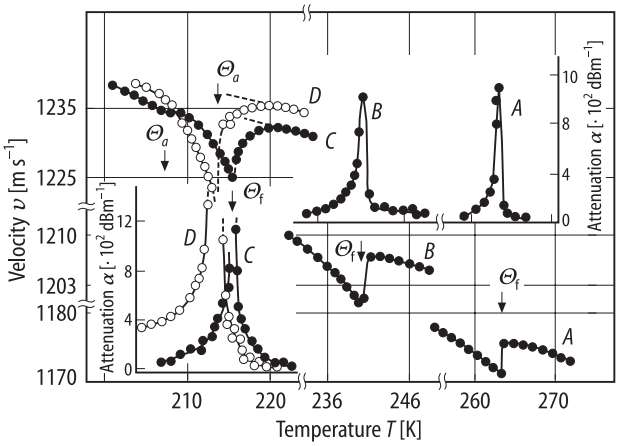

Fig. 33A-3-057. CsD_2PO_4 (DCDP). υ, α vs. T [94Kit]. Parameter: p. f = 10 MHz. υ, α: velocity and attenuation of quasi-transverse elastic wave with displacement along [100] propagating along [001] direction. *A*: p = 0.1 MPa, *B*: 280 MPa, *C*: 550 MPa, *D*: 580 MPa.

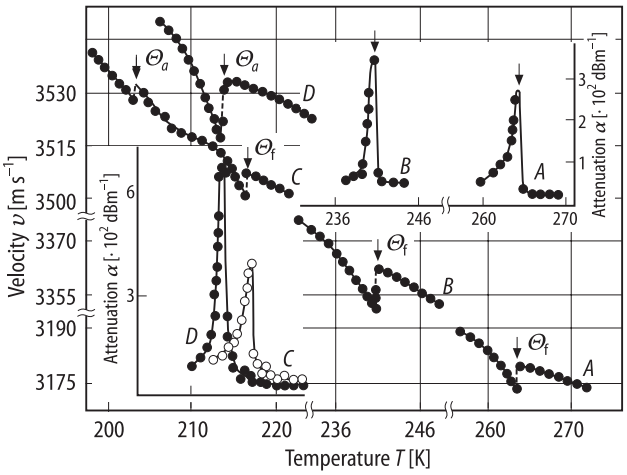

Fig. 33A-3-058. CsD_2PO_4 (DCDP). v, α vs. T [94Kit]. Parameter: p. f = 10 MHz. v, α: velocity and attenuation of quasi-longitudinal elastic wave propagating along [100] direction. *A*: p = 0.1 MPa, *B*: 280 MPa, *C*: 540 MPa, *D*: 580 MPa.

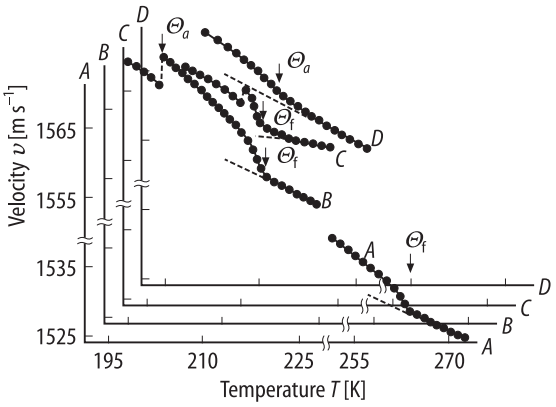

Fig. 33A-3-059. CsD_2PO_4 (DCDP). v vs. T [94Kit]. Parameter: p. f = 10 MHz. v: velocity of transverse elastic wave with displacement along [101] propagating along [010] direction. *A*: p = 0.1 MPa, *B*: 530 MPa, *C*: 560 MPa, *D*: 580 MPa.

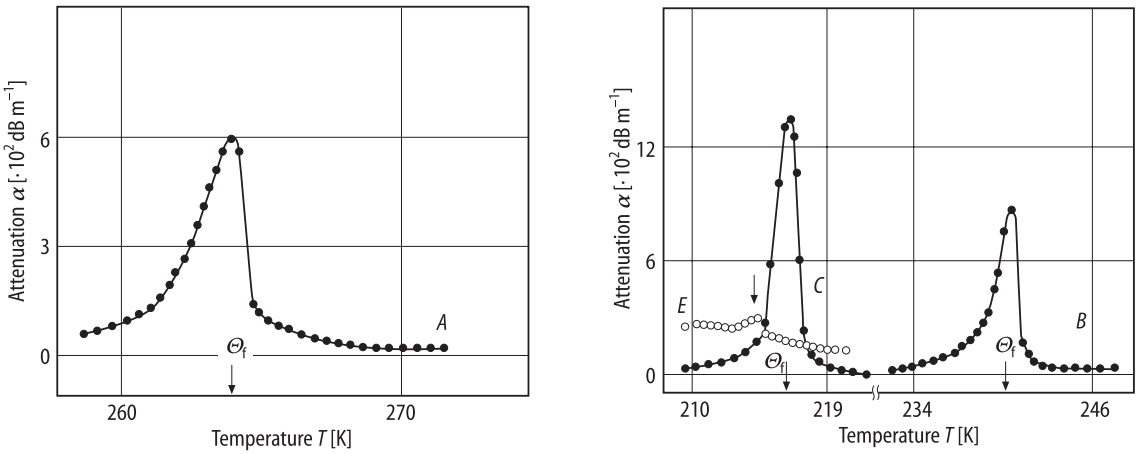

Fig. 33A-3-060. CsD_2PO_4 (DCDP). α vs. T [94Kit]. Parameter: p. f = 10 MHz. α: attenuation of longitudinal elastic wave propagating along [010] direction. *A*: p = 0.1 MPa, *B*: 280 MPa, *C*: 540 MPa, *E*: 580 MPa.

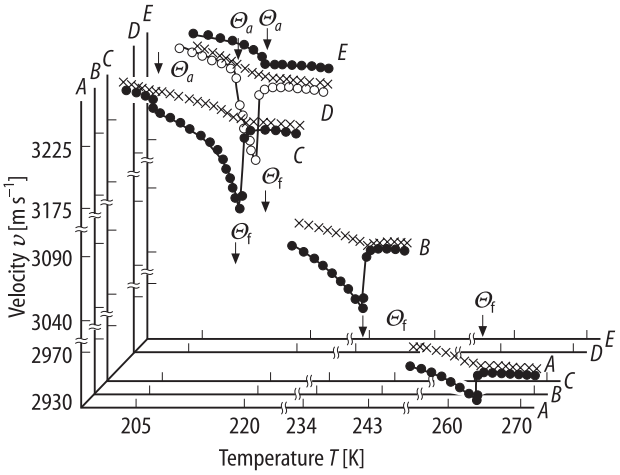

Fig. 33A-3-061. CsD_2PO_4 (DCDP). v vs. T [94Kit]. Parameter: p. f = 10 MHz. v: velocity of longitudinal elastic wave propagating along [010] direction. *A*: p = 0.1 MPa, *B*: 280 MPa, *C*: 540 MPa, *D*: 560 MPa, *E*: 580 MPa. Cross: velocity measured with applied electric field $E = 5 \cdot 10^3$ V m^{-1} along [010].

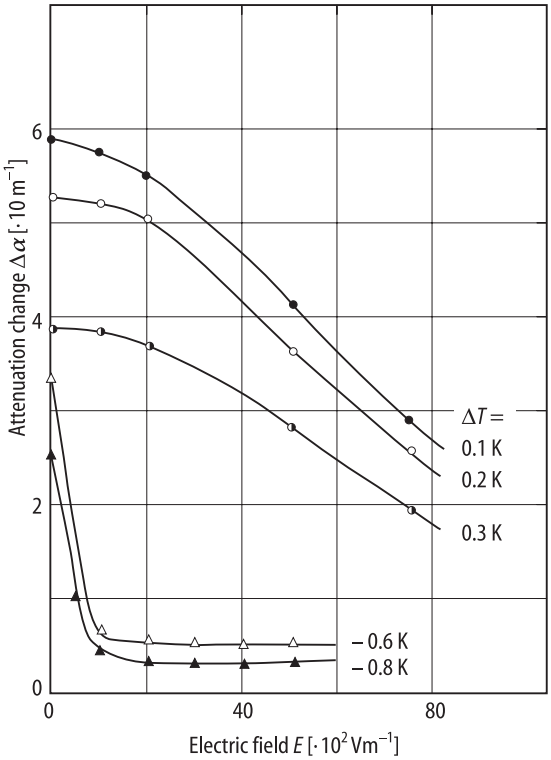

Fig. 33A-3-062. CsH_2PO_4 (CDP). $\Delta\alpha$ vs. E [93Ani]. Parameter: $\Delta T = T - \Theta_f$. $\Delta\alpha = \alpha(T, E) - \alpha(T', E)$ ($T' \gg \Theta_f$), where α is attenuation coefficient of longitudinal elastic wave propagating along *b* axis. f = 10 MHz.

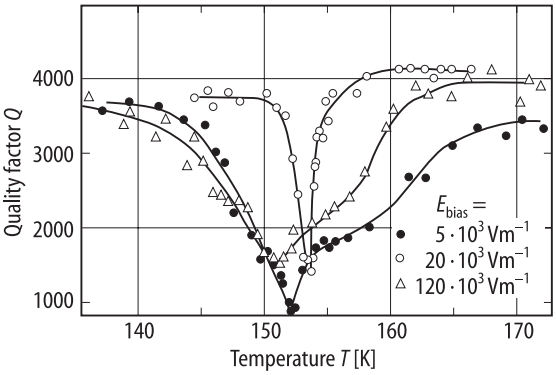

Fig. 33A-3-063. CsH_2PO_4 (CDP). Q vs. T [88Sor]. Parameter: E_{bias}. Q: mechanical quality factor. Open circle: $E_{bias} = 5 \cdot 10^3$ V m^{-1}; full circle: $20 \cdot 10^3$ V m^{-1}; open triangle: $120 \cdot 10^3$ V m^{-1}. $\boldsymbol{E}_{bias} \parallel [010]$. $f = 200$ kHz.

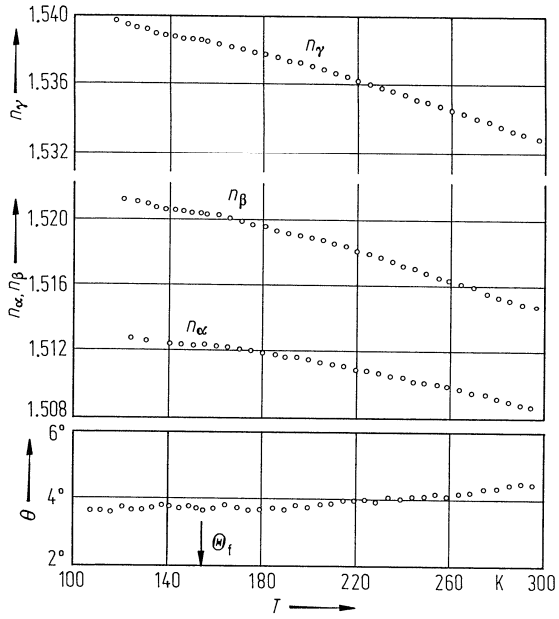

Fig. 33A-3-064. CsH_2PO_4 (CDP). n_α, n_β, n_γ, θ vs. T [84Ush]. $\lambda = 589$ nm. n_α, n_β, n_γ: principal values of the optical indicatrix. θ: rotation angle of the optical indicatrix. n_α is the value parallel to the b axis.

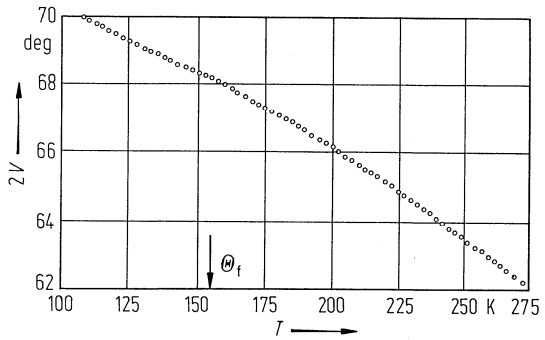

Fig. 33A-3-065. CsH_2PO_4 (CDP). $2V$ vs. T [84Ush]. $2V$: optical axial angle. $\lambda = 589$ nm.

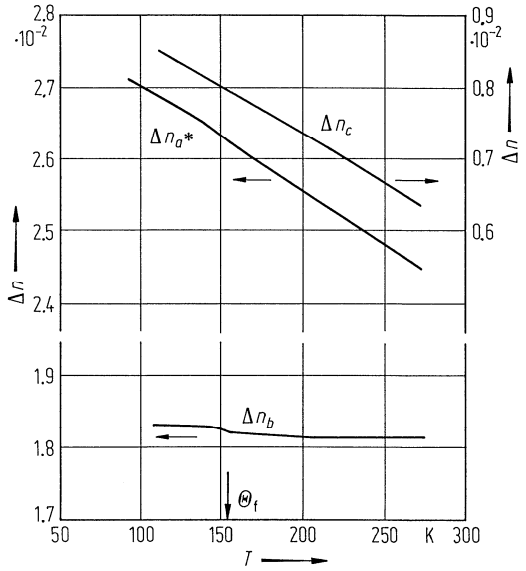

Fig. 33A-3-066. CsH_2PO_4 (CDP). Δn vs. T [84Ush]. λ = 589 nm. Δn_a, Δn_b and Δn_c are values obtained for light propagating along the $\boldsymbol{a}^*$ || $\boldsymbol{b} \times \boldsymbol{c}$, $\boldsymbol{b}$, $\boldsymbol{c}$ axes, respectively.

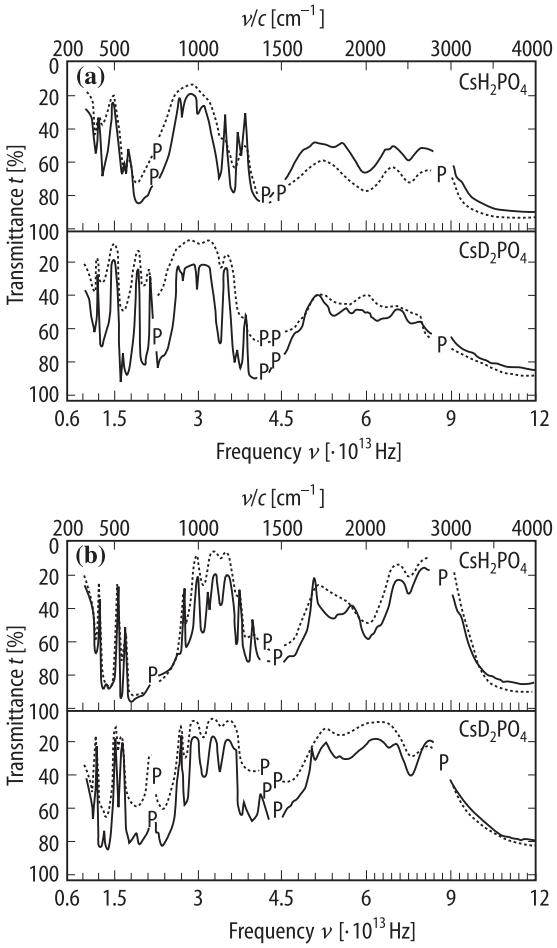

Fig. 33A-3-067. CsH_2PO_4 (CDP), CsD_2PO_4 (DCDP). t vs. ν [87Vid]. Parameter: T. t: transmittance of polarized infrared radiation measured in (100) face. (**a**) $\boldsymbol{E} \parallel \boldsymbol{b}$, (**b**) $\boldsymbol{E} \perp \boldsymbol{b}$. Solid line: T = 20 K, dashed line: T = 300 K. P: paraffin wax absorption region.

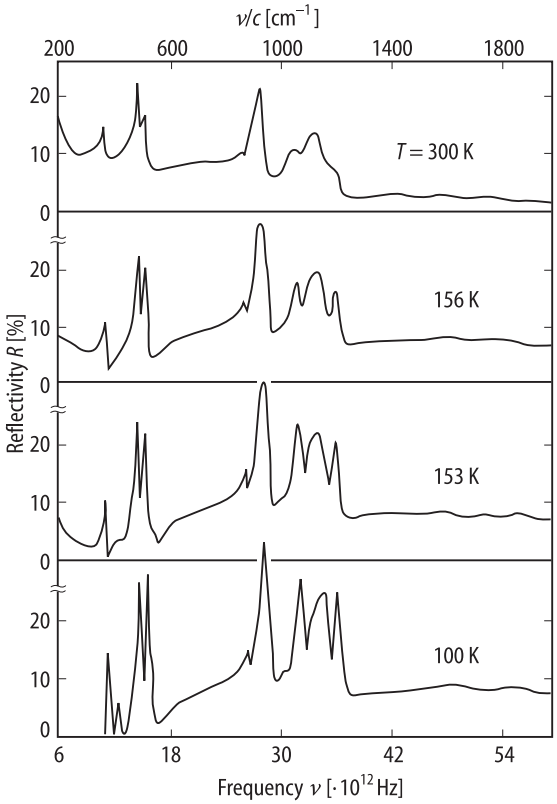

Fig. 33A-3-068. CsH_2PO_4 (CDP). R vs. ν [90Kwu]. Parameter: T. R: reflectivity. $\boldsymbol{E} \parallel \boldsymbol{b}$.

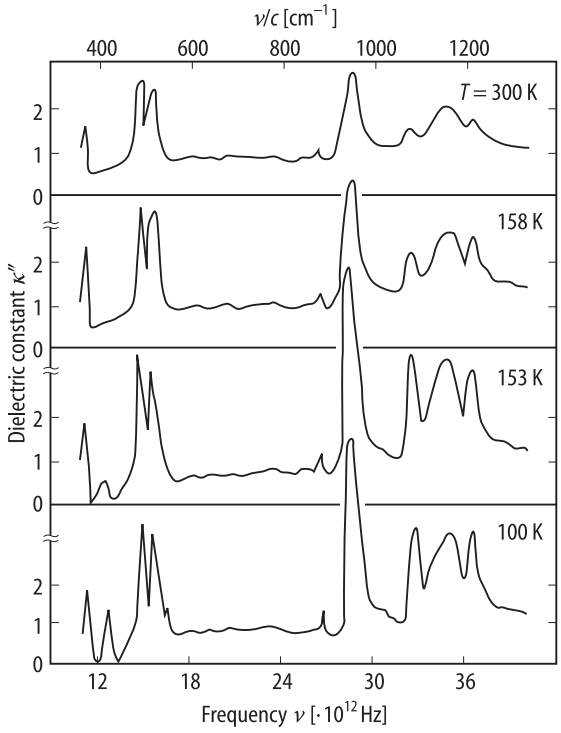

Fig. 33A-3-069. CsH_2PO_4 (CDP). κ'' vs. ν [90Kwu]. Parameter: T. $\boldsymbol{E} \perp \boldsymbol{b}$.

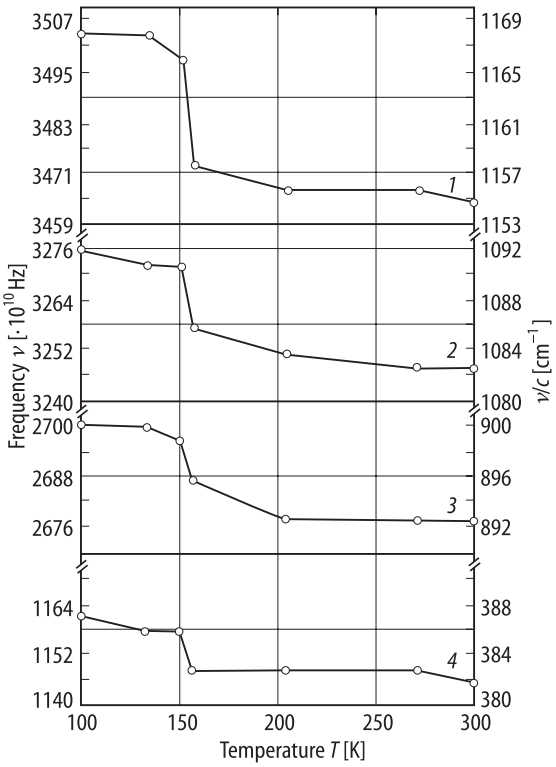

Fig. 33A-3-070. CsH_2PO_4 (CDP). ν vs. T [90Kwu]. ν: frequency of internal mode of PO_4. *1–3*: P–O stretching modes; *4*: O–P–O bending mode.

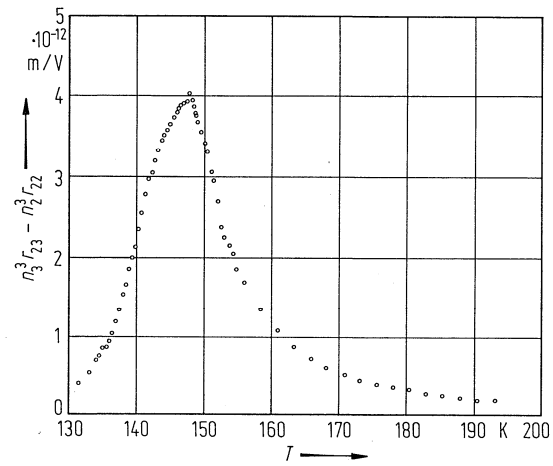

Fig. 33A-3-071. CsH_2PO_4 (CDP). $n_3^3 r_{23} - n_2^3 r_{22}$ vs. T [80Cop]. $E_{bias} = 1.8 \cdot 10^5$ V m^{-1}.

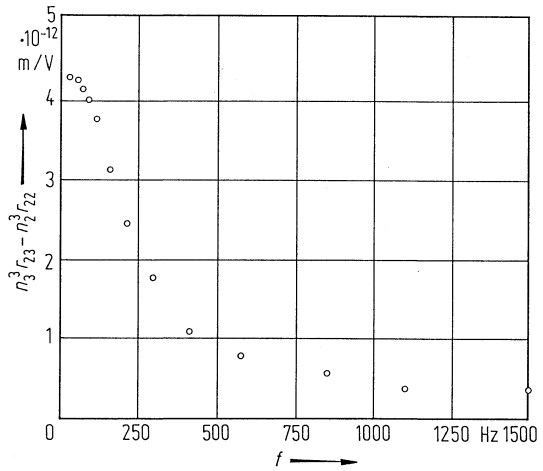

Fig. 33A-3-072. CsH_2PO_4 (CDP). $n_3^3 r_{23} - n_2^3 r_{22}$ vs. f [80Cop]. T = 147.5 K. f: frequency of applid electric field.

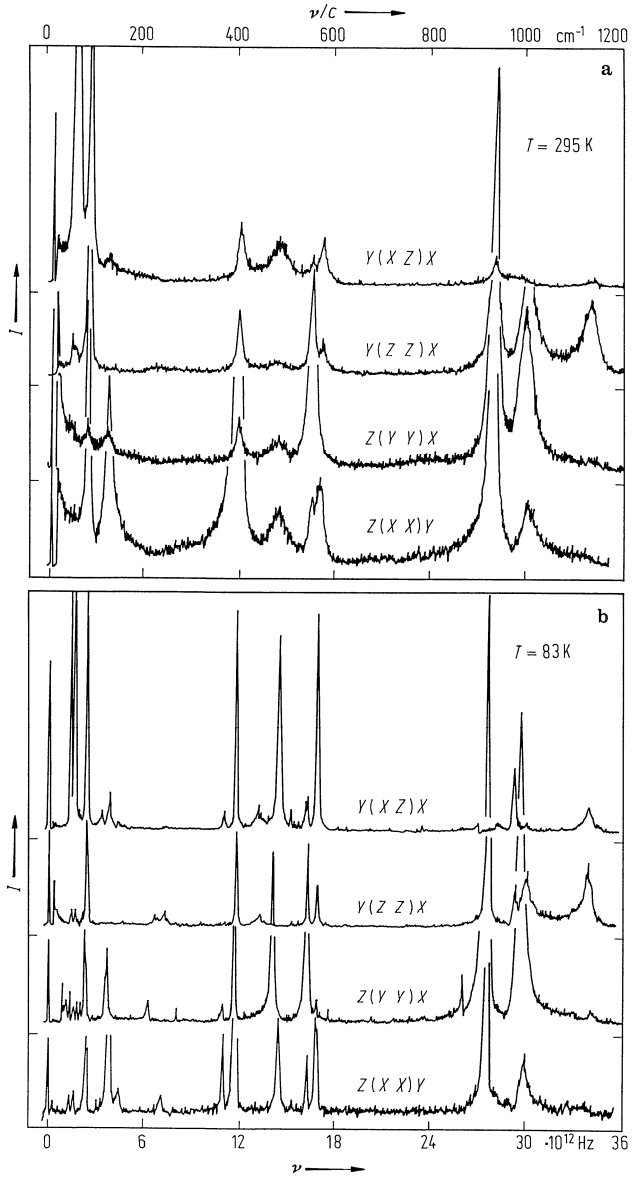

Fig. 33A-3-073. CsH_2PO_4 (CDP). *I* vs. ν at (**a**) 295 K and (**b**) 83 K for A_g and A symmetry modes [84Aok]. *I*: Raman scattering intensity. $\boldsymbol{X} \parallel \boldsymbol{a}^*$.

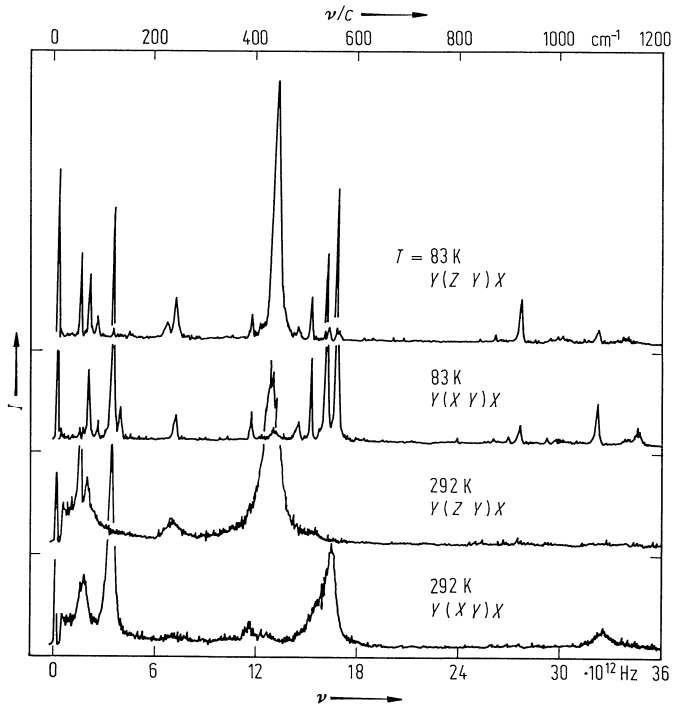

Fig. 33A-3-074. CsH_2PO_4 (CDP). *I* vs. ν at 292 K and 83 K for B_g and B symmetry modes [84Aok]. *I*: Raman scattering intensity. $\boldsymbol{X} \parallel \boldsymbol{a}^*$.

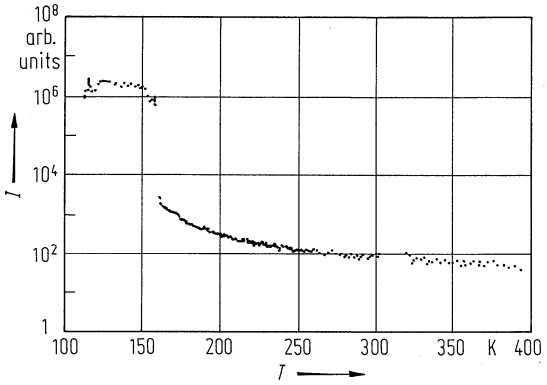

Fig. 33A-3-075. CsH_2PO_4 (CDP). *I* vs. *T* [87Shi]. *I*: intensity of a central mode measured by hyper-Raman scattering in *X*(*ZZ*)*Y* scattering geometry.

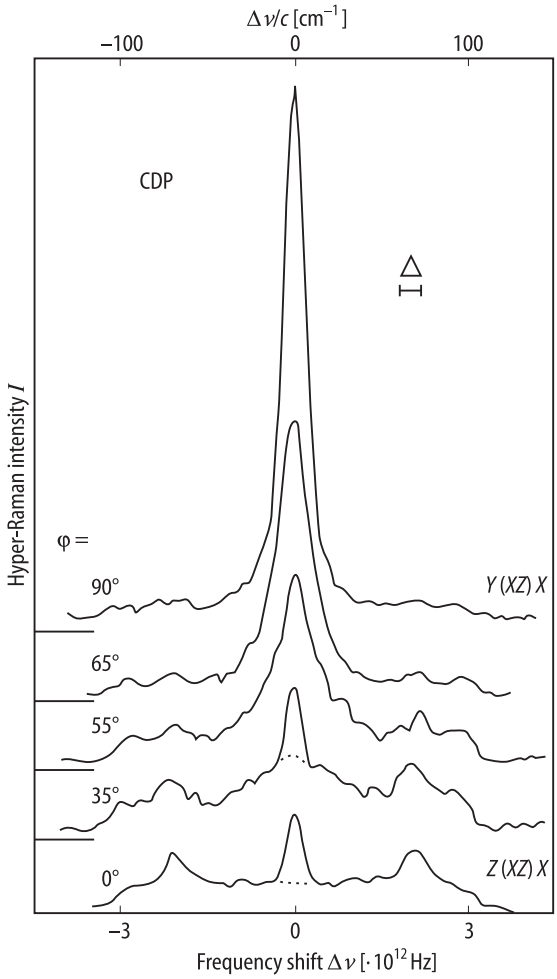

Fig. 33A-3-076. CsH_2PO_4 (CDP). I vs. $\Delta\nu$ [88Shi]. I: hyper-Raman scattering intensity. Parameter: ϕ. ϕ: angle from the b axis. T = RT.

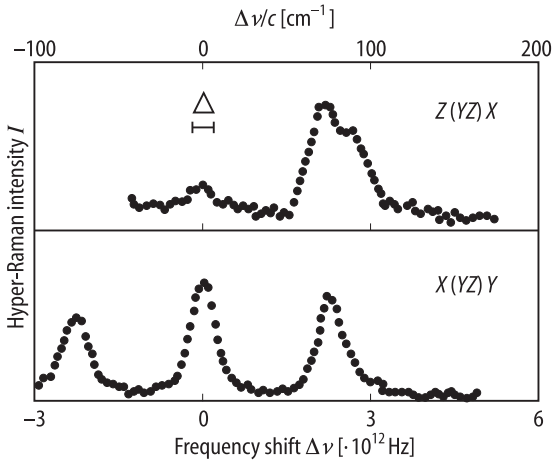

Fig. 33A-3-077. CsH_2PO_4 (CDP). I vs. $\Delta\nu$ [88Shi]. I: hyper-Raman scattering intensity. T = RT.

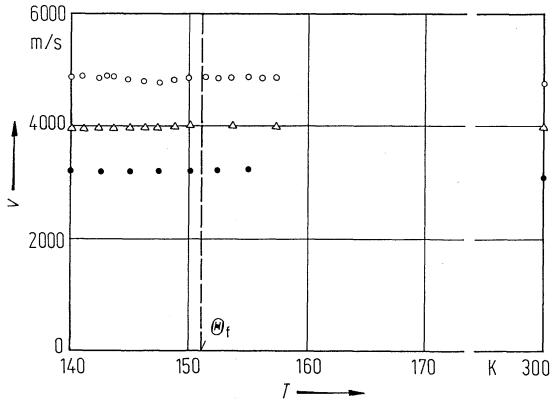

Fig. 33A-3-078. CsH_2PO_4 (CDP). v vs. T [81Mar]. Parameter: q. q: phonon wave vector. v: velocity of longitudinal acoustic phonons measured by Brillouin scattering. Open circle: $\boldsymbol{q}$ || [1, 0, 0]; full circle: $\boldsymbol{q}$ || [0, 1, 0]; open triangle: quasi-longitudinal wave, $\boldsymbol{q}$ || [–1/2, –1/2, $-1/\sqrt{2}$].

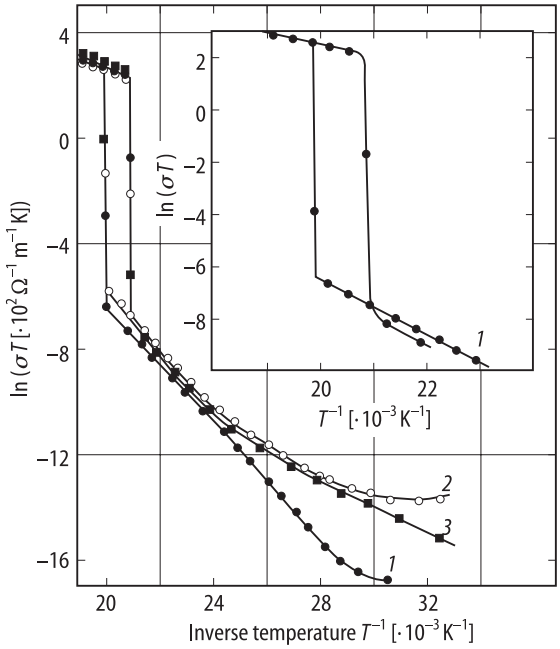

Fig. 33A-3-079. CsH_2PO_4 (CDP). ln (σT) vs. T^{-1} [88Bar]. σ: electrical conductivity in units of 10^2 Ω^{-1} m^{-1}. T: temperature in units of K. *1*: *a* direction, *2*: *b* direction, *3*: *c* direction.

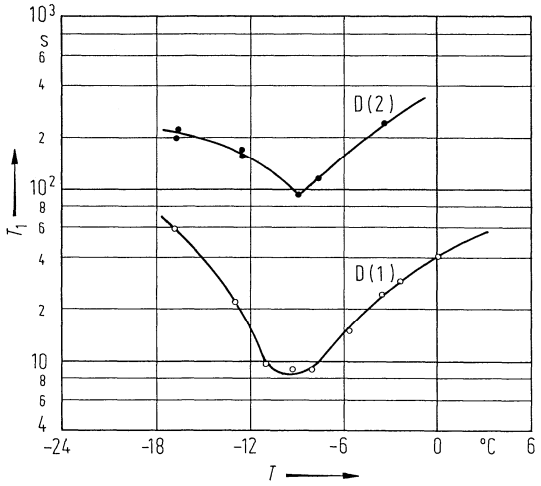

Fig. 33A-3-080. CsD_2PO_4 (DCDP). T_1 vs. T [80Top]. T_1: deuteron spin-lattice relaxation time. ν_L = 41.45 MHz, $\boldsymbol{H} \parallel \boldsymbol{c}$.

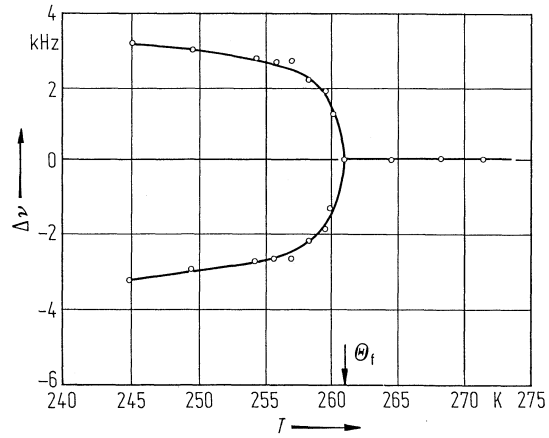

Fig. 33A-3-081. CsD_2PO_4 (DCDP). $\Delta\nu$ vs. T [80Top]. $\Delta\nu$: quadrupole splitting of O–D(1)...O deuteron NMR line. ν_L = 13.8 MHz.

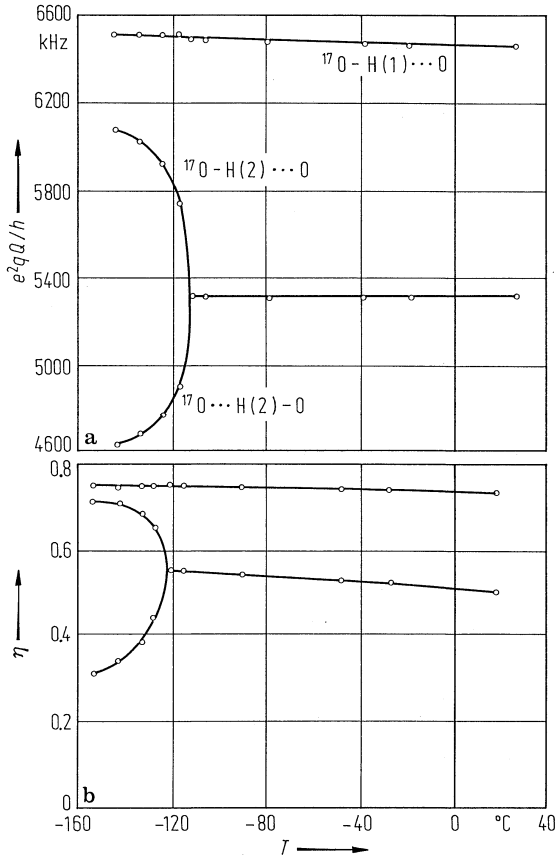

Fig. 33A-3-082. CsH_2PO_4 (CDP). ^{17}O NQR [84Sel]. (**a**) e^2qQ/h vs. *T*. (**b**) η vs. *T*. η: asymmetry parameter.

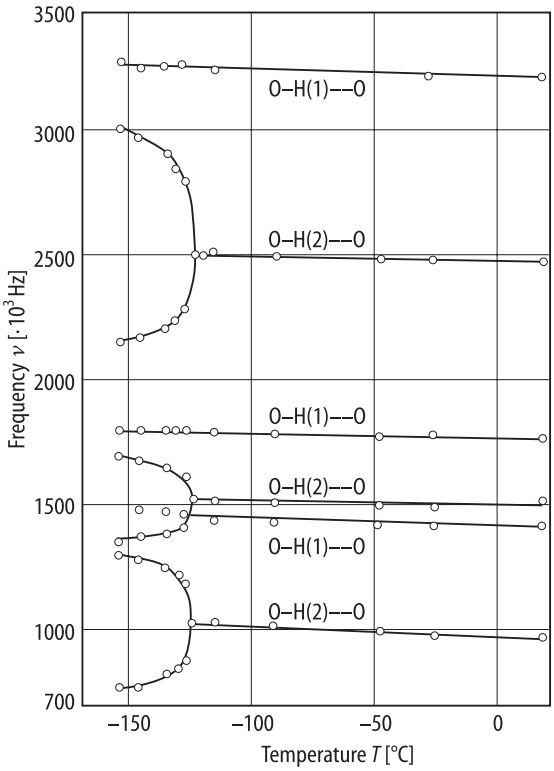

Fig. 33A-3-083. CsH_2PO_4 (CDP). ν vs. T [86Bli, 84Sel]. ν: ^{17}O NQR frequency.

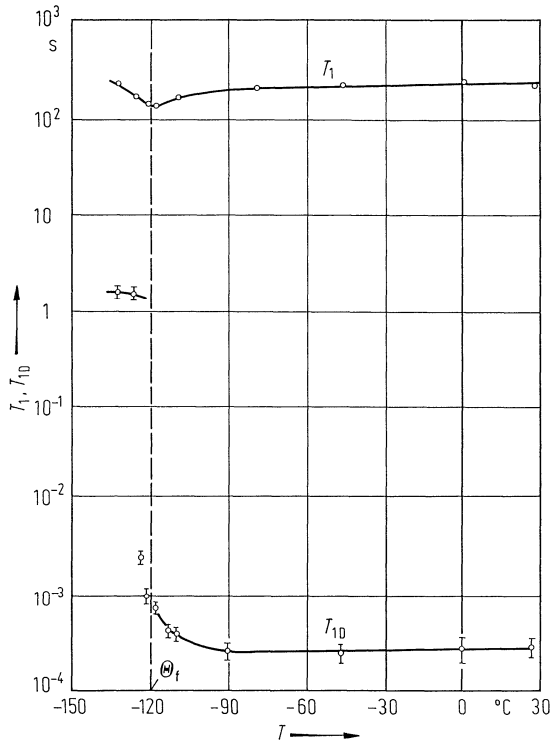

Fig. 33A-3-084. CsH_2PO_4 (CDP). T_1, T_{1D} vs. T [80Sla]. T_1: ^{31}P spin-lattice relaxation time. T_{1D}: ^{31}P spin-lattice relaxation time in dipolar field. $\boldsymbol{H} \parallel \boldsymbol{c}$, ν_L = 23.8 MHz.

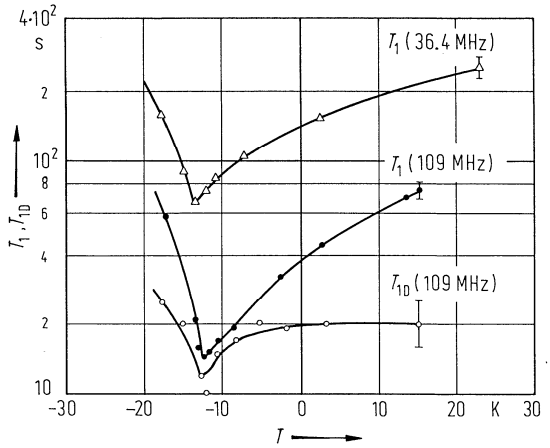

Fig. 33A-3-085. CsD_2PO_4 (DCDP). T_1, T_{1D} vs. T [80Bli]. T_1: ^{31}P spin-lattice relaxation time. T_{1D}: ^{31}P spin-lattice relaxation time in dipolar field. $\boldsymbol{H} \parallel \boldsymbol{c}$.

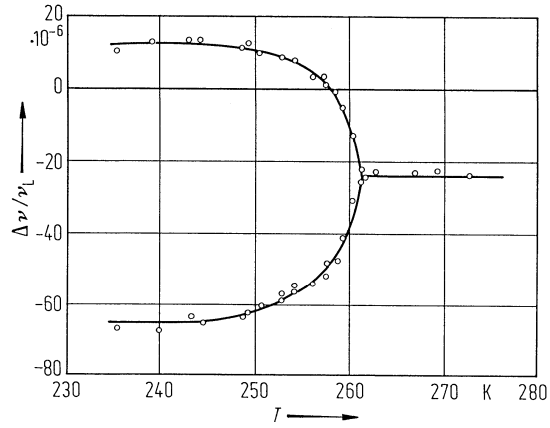

Fig. 33A-3-086. CsD_2PO_4 (DCDP). $\Delta\nu/\nu_L$ vs. T [80Bli]. $\Delta\nu$: ^{31}P chemical shift splitting. ν_L = 109.3 MHz.

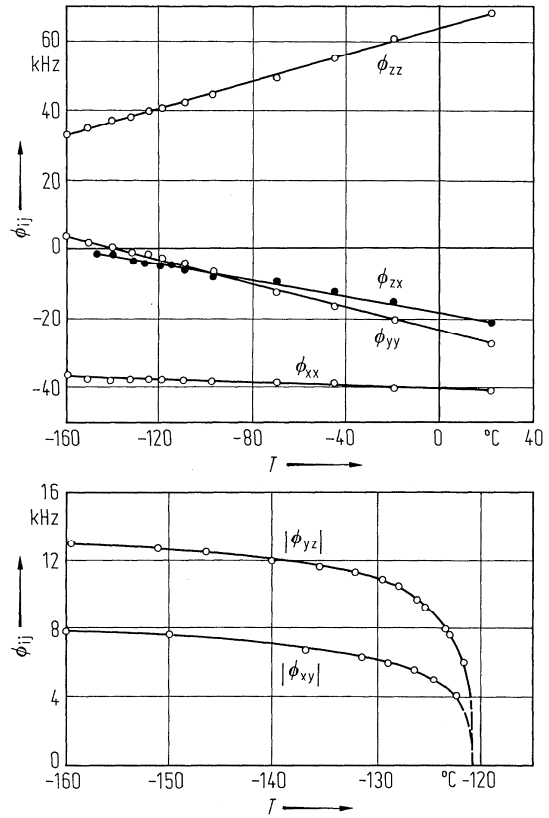

Fig. 33A-3-087. CsH_2PO_4 (CDP). ϕ_{ij} vs. T [77Kan]. ϕ_{ij}: electric field gradient tensor components of ^{133}Cs. $\boldsymbol{x} \perp \boldsymbol{b}$, $\boldsymbol{z} \parallel \boldsymbol{c}$.

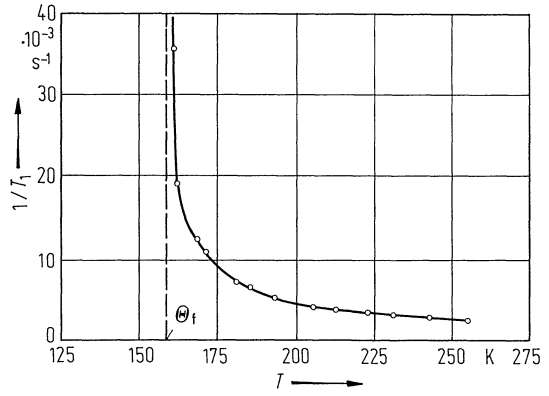

Fig. 33A-3-088. CsH_2PO_4 (CDP). T_1^{-1} vs. T [83Bli]. T_1: ^{133}Cs spin-lattice relaxation time. ν_L = 8.8 MHz. $\boldsymbol{H} \perp \boldsymbol{c}$. $\angle(\boldsymbol{H}, \boldsymbol{a}) = 90°$.

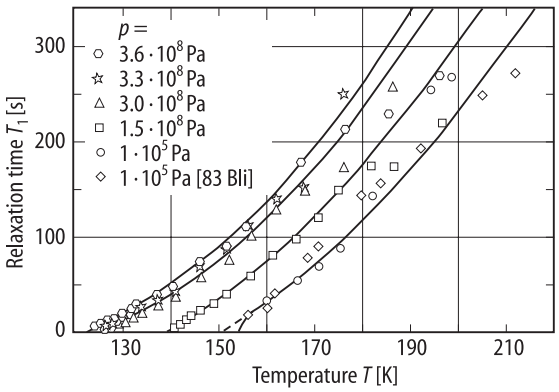

Fig. 33A-3-089. CsH_2PO_4 (CDP). T_1 vs. T [89Sch]. Parameter: p. T_1: ^{133}Cs spin-lattice relaxation time.

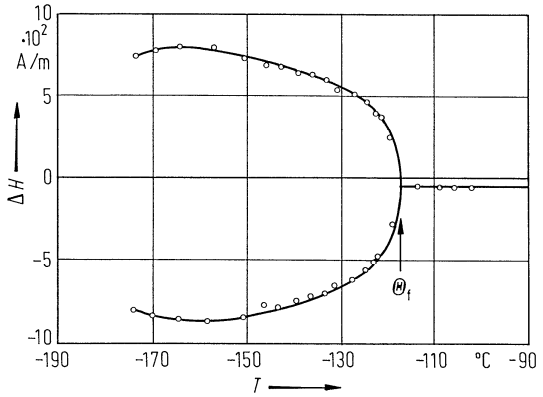

Fig. 33A-3-090. CsH_2PO_4 (CDP). ΔH vs. T [85Bli]. ΔH: splitting of Tl^{2+} doublet. $\boldsymbol{H} \perp \boldsymbol{b}$; $\angle(\boldsymbol{H}, \boldsymbol{c}) = 25°$.

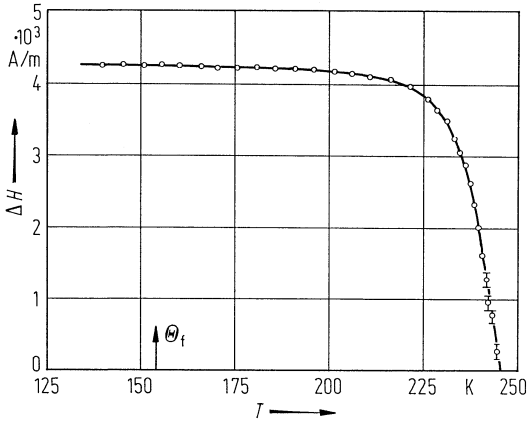

Fig. 33A-3-091. CsH_2PO_4 (CDP). ΔH vs. T [84Wap]. ΔH: $(CrO_4)^{3-}$ ESR line splittinig. $\boldsymbol{H} \parallel [110]$.

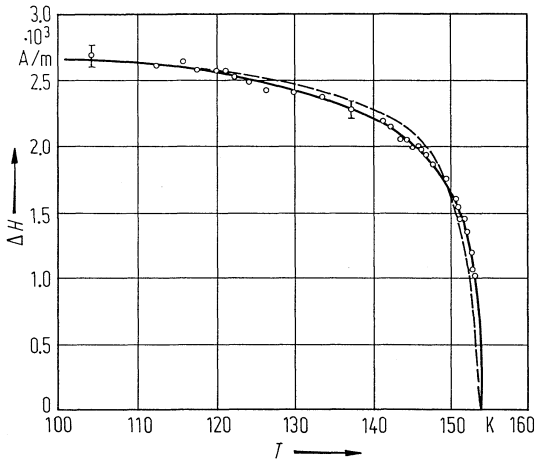

Fig. 33A-3-092. CsH_2PO_4 (CDP). ΔH vs. T [80Tak]. ΔH: line splitting for $(AsO_3)^{2-}$ radical. $\nu_L = 9 \cdot 10^{10}$ Hz. Dashed line: spontaneous polarization obtained from D–E hysteresis loop.

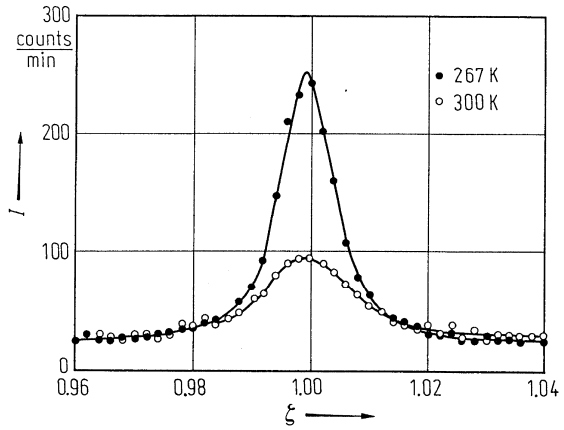

Fig. 33A-3-093. CsD_2PO_4 (DCDP). I vs. ζ [77Sem]. I: neutron scattering intensity at (2.15, ζ, 0).

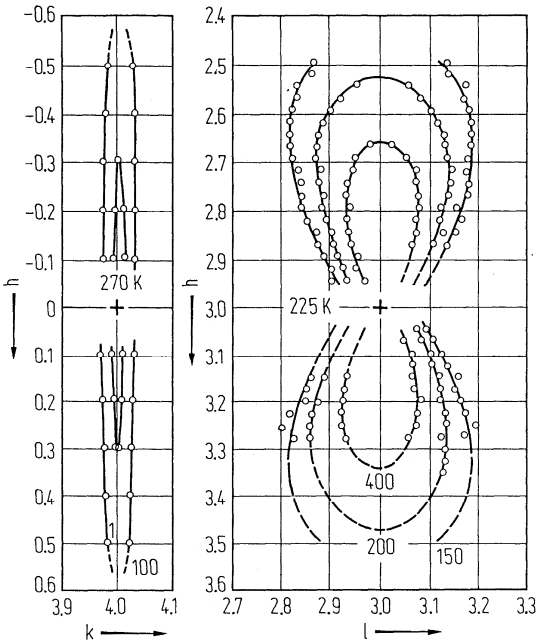

Fig. 33A-3-094. CsD_2PO_4 (DCDP), KD_2PO_4 (DKDP). Neutron scattering intensity contours [77Sem]. (**a**) Contours in the (h k 0) zone near (0 4 0) for CsD_2PO_4 at T = 270 K. (**b**) Contours in the (h 0 l) zone near (3 0 3) for KD_2PO_4 at T = 225 K. The figures are drawn to the same scale in inverse. The intensity units are arbitrary. See also [70Ska].

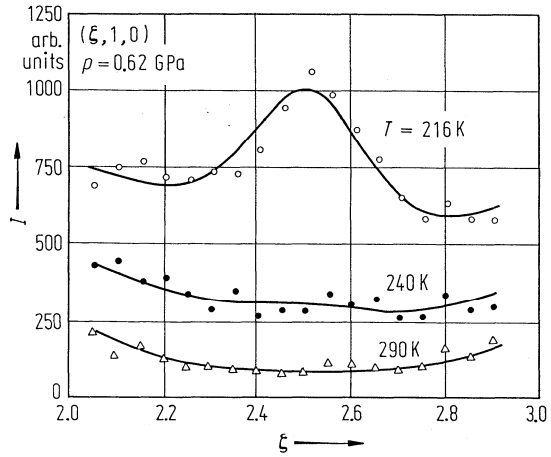

Fig. 33A-3-095. CsD_2PO_4 (DCDP). I vs. ζ at p = 0.62 GPa [80You]. I: neutron diffuse scattering intensity at (ζ, 1, 0). Parameter: T.

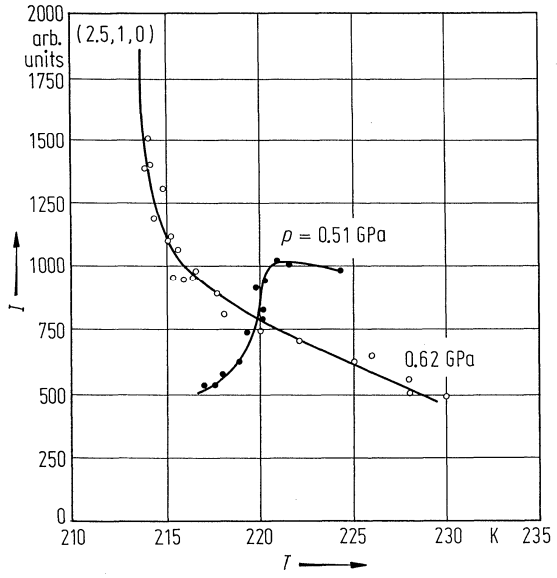

Fig. 33A-3-096. CsD_2PO_4 (DCDP). *I* vs. *T* [80You]. *I*: neutron diffuse scattering intensity at (2.5, 1, 0). Parameter: *p*.

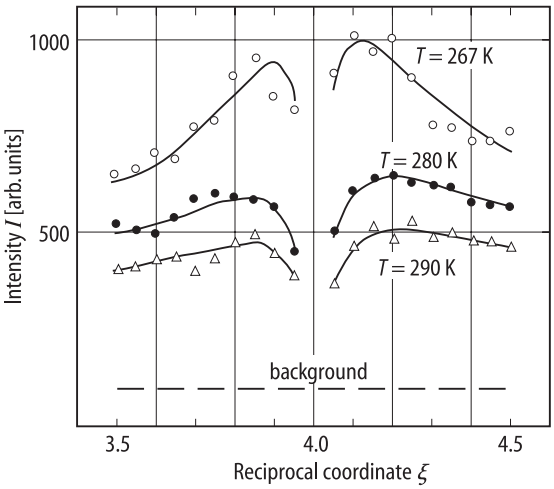

Fig. 33A-3-097. CsD_2PO_4 (DCDP). *I* vs. ξ [80You]. Parameter: *T*. *I*: neutron diffuse scattering intensity parallel to a^* in the reciprocal space around (4, 3, 0).

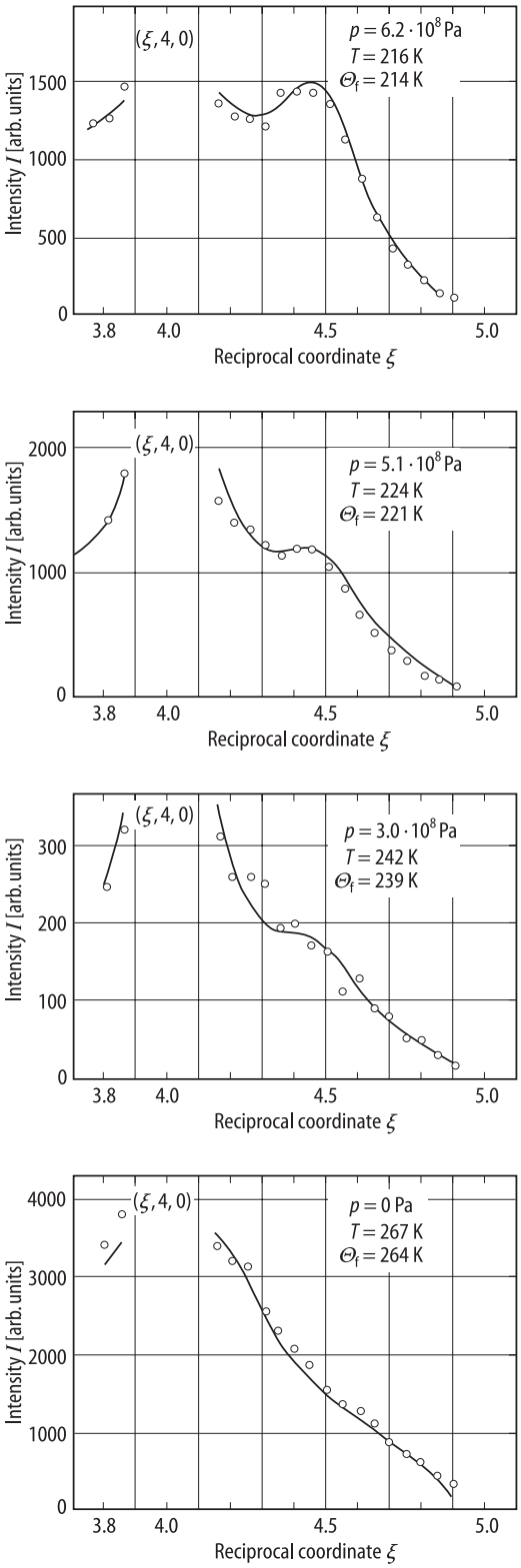

Fig. 33A-3-098. CsD_2PO_4 (DCDP). I vs. ξ [80You]. Parameters: T, p. I: neutron diffuse scattering intensity at (ξ, 4, 0) in the reciprocal space around (0, 4, 0). $T - \Theta_f$ are held approximately constant. Data for $p = 0$ are from [79Fra].

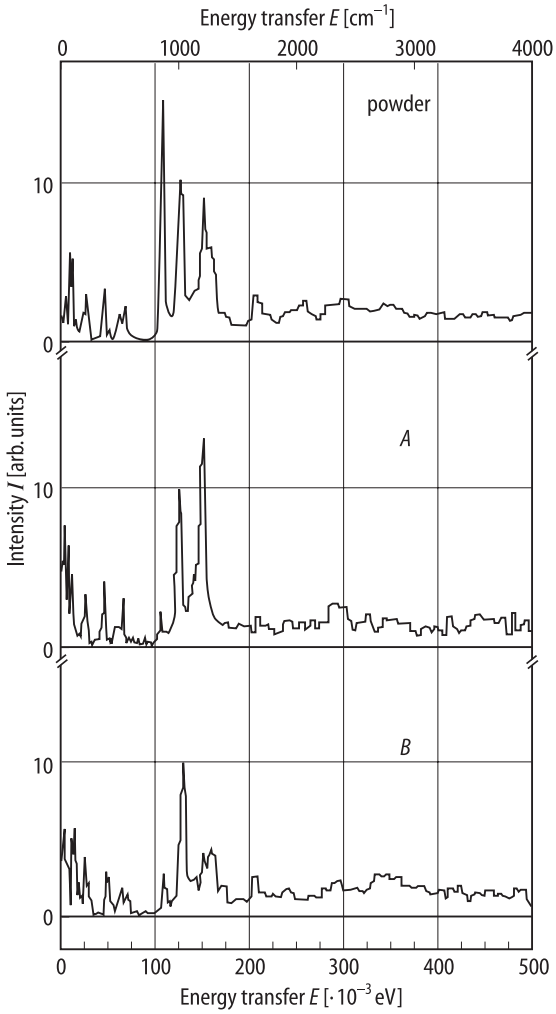

Fig. 33A-3-099. CsH_2PO_4 (CDP). I vs. E [89Fil]. I: inelastic neutron scattering intensity. E: energy transfer. T = 20 K. A: single crystals with the incident beam perpendicular to [001]; B: single crystal, incident beam perpendicular to [100].

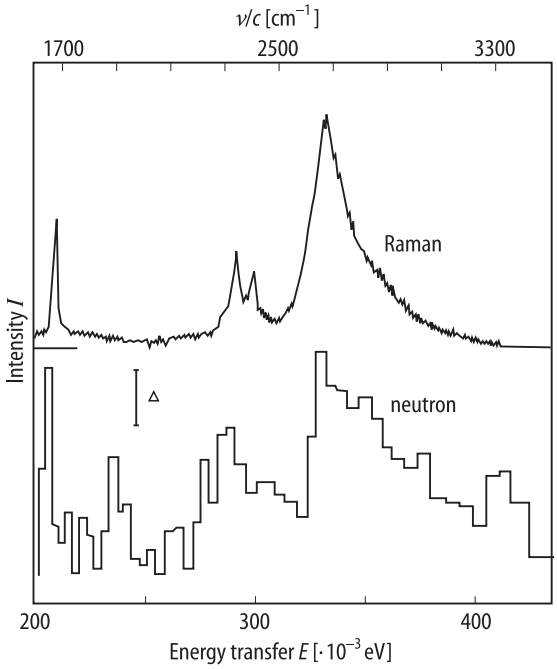

Fig. 33A-3-100. CsH_2PO_4 (CDP). *I* vs. *E* [89Fil]. *I*: inelastic neutron scattering intensity in the OH stretching region of the long hydrogen bond along the *c* axis. *E*: energy transfer. $T = 20$ K. Δ: instrumental error for neutron scattering. Raman spectrum is indicated for comparison.

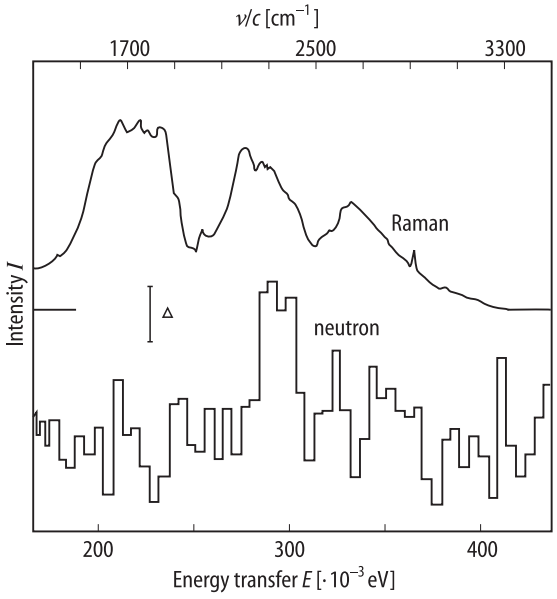

Fig. 33A-3-101. CsH_2PO_4 (CDP). *I* vs. *E* [89Fil]. *I*: inelastic neutron scattering intensity in the OH stretching region of the short hydrogen bond along the *a** axis. *E*: energy transfer. $T = 20$ K. Δ: instrumental error for neutron scattering. Raman spectrum is indicated for comparison.

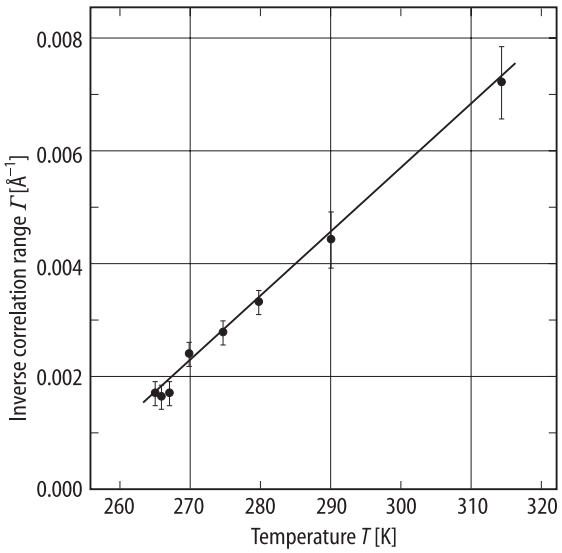

Fig. 33A-3-102. CsH_2PO_4 (CDP). Γ vs. T [79Fra]. Γ: intrachain inverse correlation range determined from neutron scattering in (h k 0) zone.

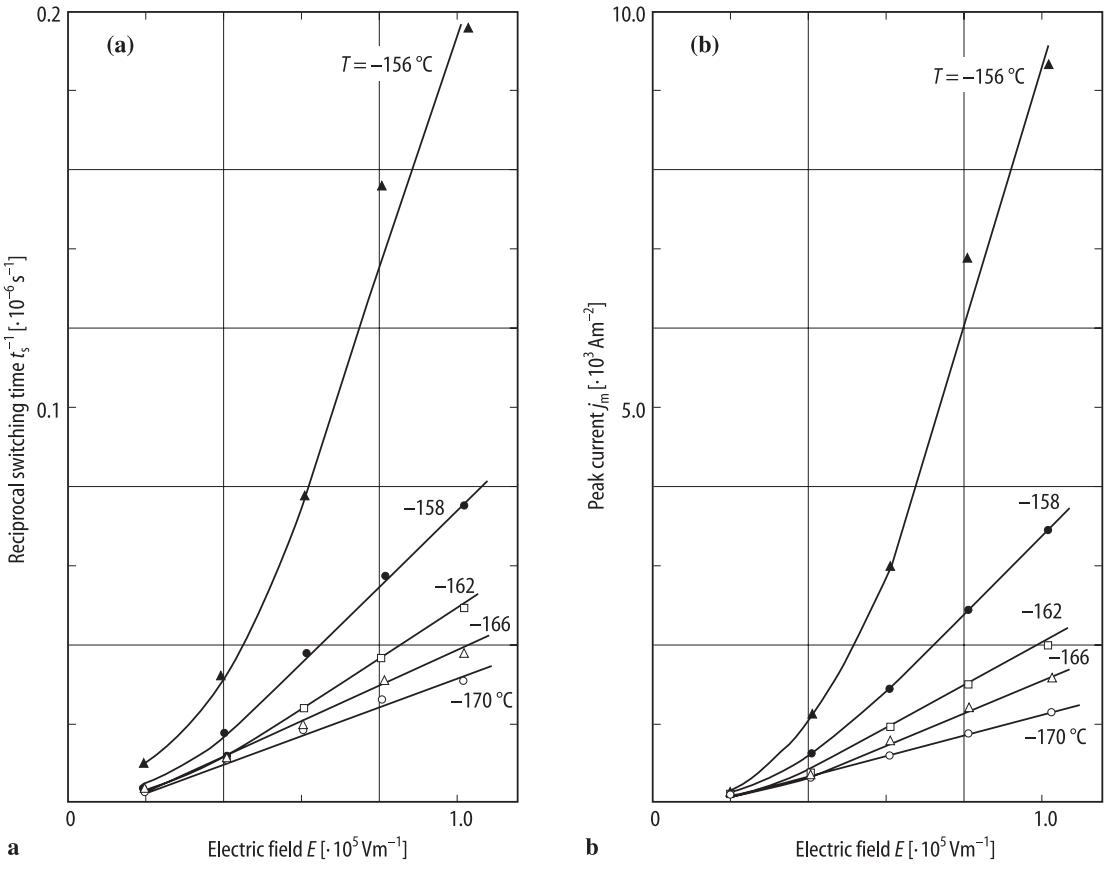

Fig. 33A-3-103. CsH_2PO_4 (CDP). t_s^{-1}, j_m vs. E in the pressure induced antiferroelectric phase [79Yas2]. Parameter: T. t_s: switching time. j_m: maximum switching current density. E: applied electric field. $p = 4 \cdot 10^8$ Pa.

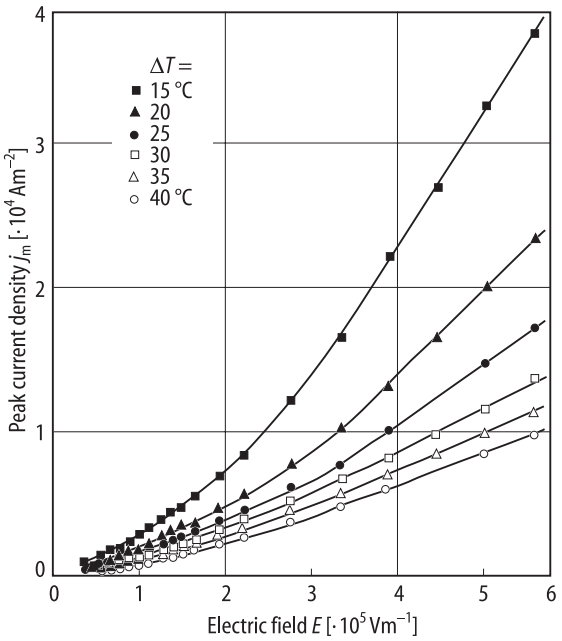

Fig. 33A-3-104. CsH_2PO_4 (CDP). j_m vs. E [83Fuj]. Parameter: $\Delta T = \Theta_f - T$. j_m: maximum switching current density.

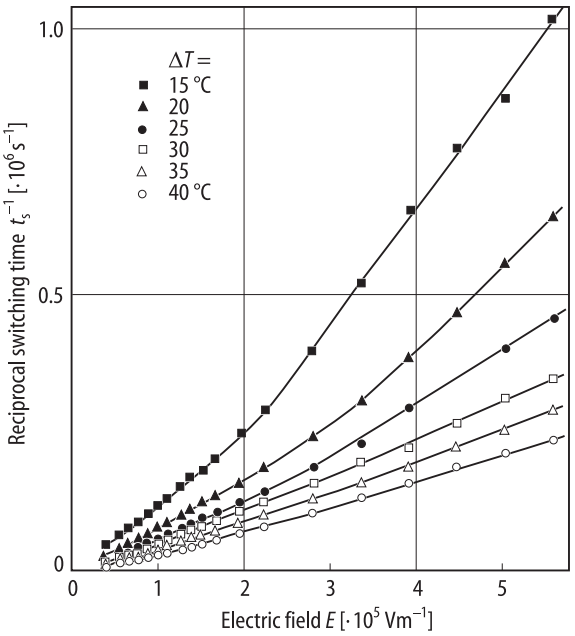

Fig. 33A-3-105. CsH_2PO_4 (CDP). t_s^{-1} vs. E [83Fuj]. Parameter: $\Delta T = \Theta_f - T$. t_s: switching time.